Receptor Models: the quantification of air pollution sources from in situ measurements

Maria de Fatima Andrade

IAG-USP

Outline

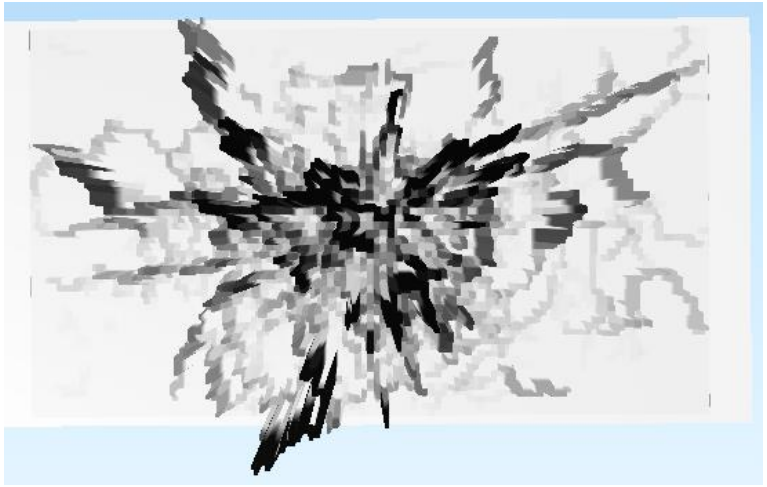

- Introduction: motivation to use Receptor Models
- Examples of urban and industrial cases
- Methods
  - CMB
  - ACP, FA
  - PMF
  - Final Remarks
  - Questions

Dispersion Models

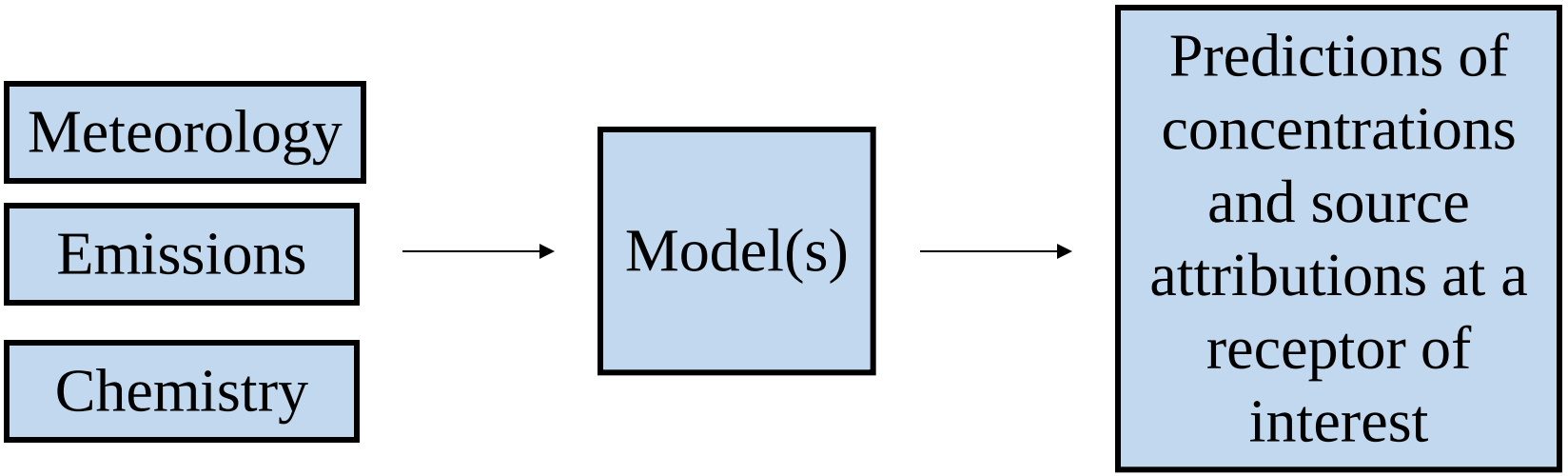

Examples

-SMOKE (Emissions Model)

-CMAQ (Air Quality Models)

-WRF – Chem , Chemical Transport Models

Receptor Models

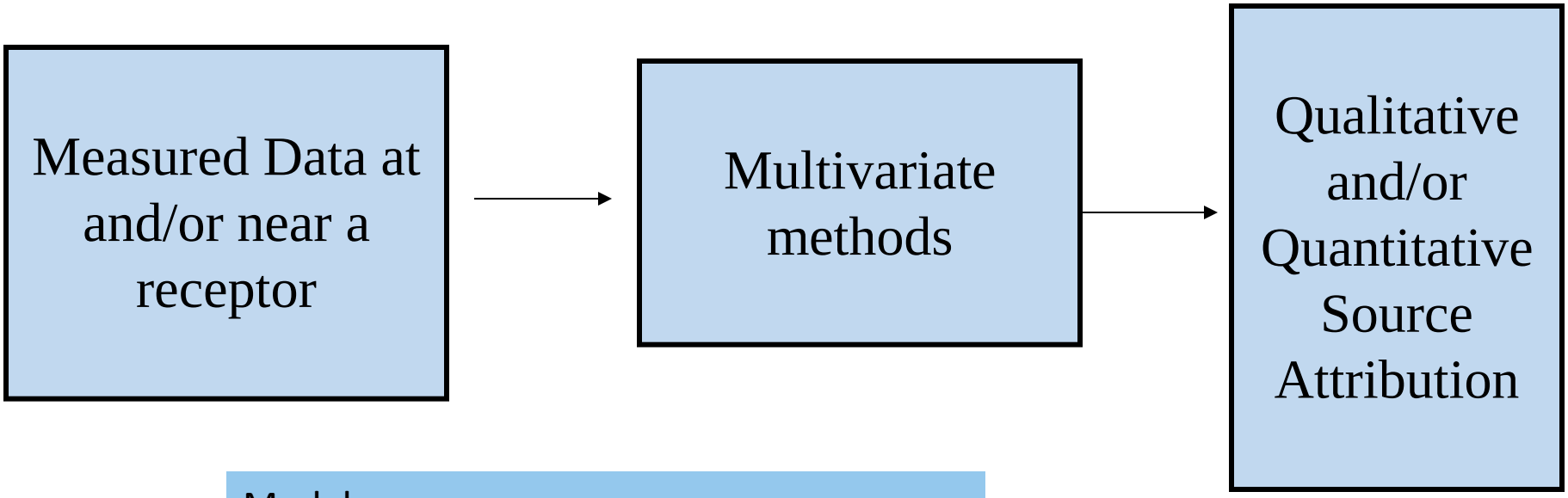

Models:

CMB, Chemical Mass Balance

PCA, Principal Component Analysis

PMF, Positive Matrix Factorization

Chemical Mass Balance Model (CMB8.2)

- A **receptor model** source apportionment using ambient data and source profile data with appropriate uncertainty estimates.

- Version 8.2 available at EPA Support Center for Regulatory Air Models - http://www.epa.gov/ttn/scram/receptor_cmb.htm

Principles

- A solution to linear equations that express each receptor chemical concentration as a linear sum of products of **source profile abundances** and **source contributions**.
- **Mass and chemical compositions** of source emissions are conserved from the time of emission to the time the sample is taken.

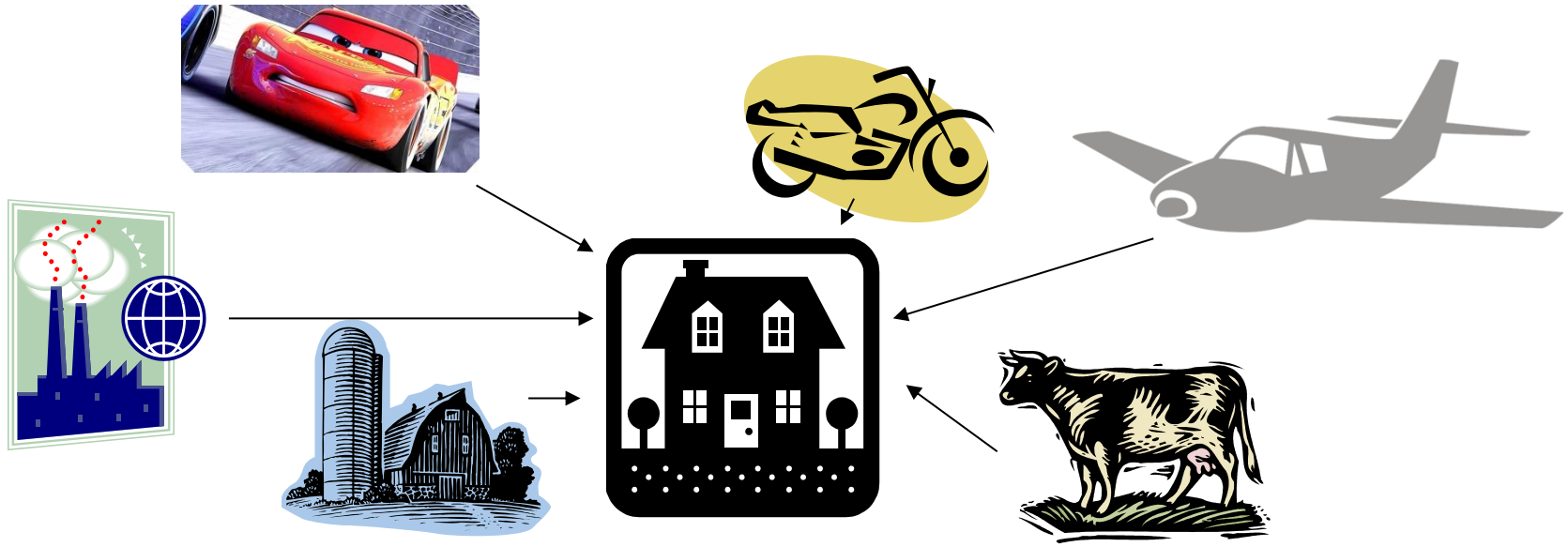

EPRI

Modeling Procedures

- Identify the types of contributing sources
- Select chemical species or other properties to be included in the calculation
- Determine the fraction of each of the chemical species which is contained in each source type (source profiles)
- Estimate the uncertainty in both ambient concentrations and source profiles
- Solve the chemical mass balance equations

Chemical Mass Balance

Equation:

$$C_i = \sum_{j=1}^{J} F_{ij} \; S_j \qquad \text{for } i = 1 \text{ to } N$$

Input:

- Ambient Concentrations (C_i)
  uncertainties in ambient concentrations (σ_{Cj}),
  Source Profiles(F_{ij}),
  uncertainties in source profiles (σ_{Fij}).

Output:

- Source contributions (S_j)
  and uncertainties (σ_{Sj}).

Measurements:

- Size-classified mass, elements, ions, and carbon concentrations at ambient and source samples.

Mininum Square Solution

- The general equation has the objective of minimize the sum of quadratic deviation:

$$\chi^2 = \sum_i \frac{\left[C_i - \sum_j F_{ij} S_j \right]^2}{\sigma^2{}_i}$$

- Minimize χ^2 is to determiene Sk that

$$\frac{\partial \chi^2}{\partial S_k} = 0$$

$$\frac{\partial \chi^2}{\partial S_K} = -2\sum_i \left[C_i - \sum_j F_{ij} S_j \right] F_{iK}$$

$$\sum_i C_i F_{ik} - \sum_j S_j \sum_i F_{ij} F_{ik} = 0$$

In Matricial form the equation is :

$$\mathbf{F}^t\mathbf{C} = \mathbf{F}^t\,\mathbf{FS}$$

$$\mathbf{C} = \begin{bmatrix} C_1 \\ C_2 \\ \\ C_n \end{bmatrix} \qquad \mathbf{S} = \begin{bmatrix} S_1 \\ S_2 \\ \\ S_m \end{bmatrix} \qquad \mathbf{F} = \begin{bmatrix} F_{11} & F_{12} & & F_{1m} \\ F_{21} & F_{22} & & F_{2m} \\ & & F_{ij} & \\ F_{n1} & F_{n2} & & F_{nm} \end{bmatrix}$$

n = number of elements m = number of sources

Effective Variance Weighted Linear Least Square Method

- minimizing χ^2 (difference between measured value, c_i, and calculated value, $F_{ij}S_j$, weighed by analytical uncertainty)

$$\chi^2 = \frac{1}{I-J}\sum_{i=1}^{I}\left[\left(\mathbf{C_i} - \sum_{j=1}^{J}\mathbf{F_{ij}S_j}\right)^2 / \mathbf{V_{e_{ij}}}\right]$$

where the denominator is called **effective variance**

$$\mathbf{V_{e_{ij}}} = \sigma_{C_i}^2 + S_j^2 \cdot \sigma_{F_{ij}}^2$$

σ_{C_i} Standard deviation uncertainty of the C_i measurement

$\sigma_{F_{ij}}$ Standard deviation uncertainty of the F_{ij} measurement

- The solution in matrix form is

$$\mathbf{S} = \left(\mathbf{F}^{\mathbf{T}}\mathbf{V}_{\mathbf{e}}^{-\mathbf{1}}\mathbf{F}\right)^{-\mathbf{1}}\mathbf{F}^{\mathbf{T}}\mathbf{V}_{\mathbf{e}}^{-\mathbf{1}}\mathbf{C}$$

- S_j is initially set to 0. An iterative procedure is applied until S_j does not change more than 1% from step to step (k → k+1)

$$\left|\left(S_j^{k+1} - S_j^{k}\right) / S_j^{k+1}\right| \leq 0.01$$

Examples

Contents lists available at SciVerse ScienceDirect
Atmospheric Environment
journal homepage: www.elsevier.com/locate/atmosenv

Review

Critical review and meta-analysis of ambient particulate matter source apportionment using receptor models in Europe

C.A. Belis [a,*], F. Karagulian [a], B.R. Larsen [b], P.K. Hopke [c]

[a] European Commission, Joint Research Centre, Institute for Environment and Sustainability, Via Enrico Fermi 2749, Ispra (VA) 21027, Italy
[b] European Commission, Joint Research Centre, Institute for Health and Consumer Protection, Via Enrico Fermi 2749, Ispra (VA) 21027, Italy
[c] Center for Air Resources Engineering and Science, Clarkson University, Box 5708, Potsdam, NY 13699-5708, United States

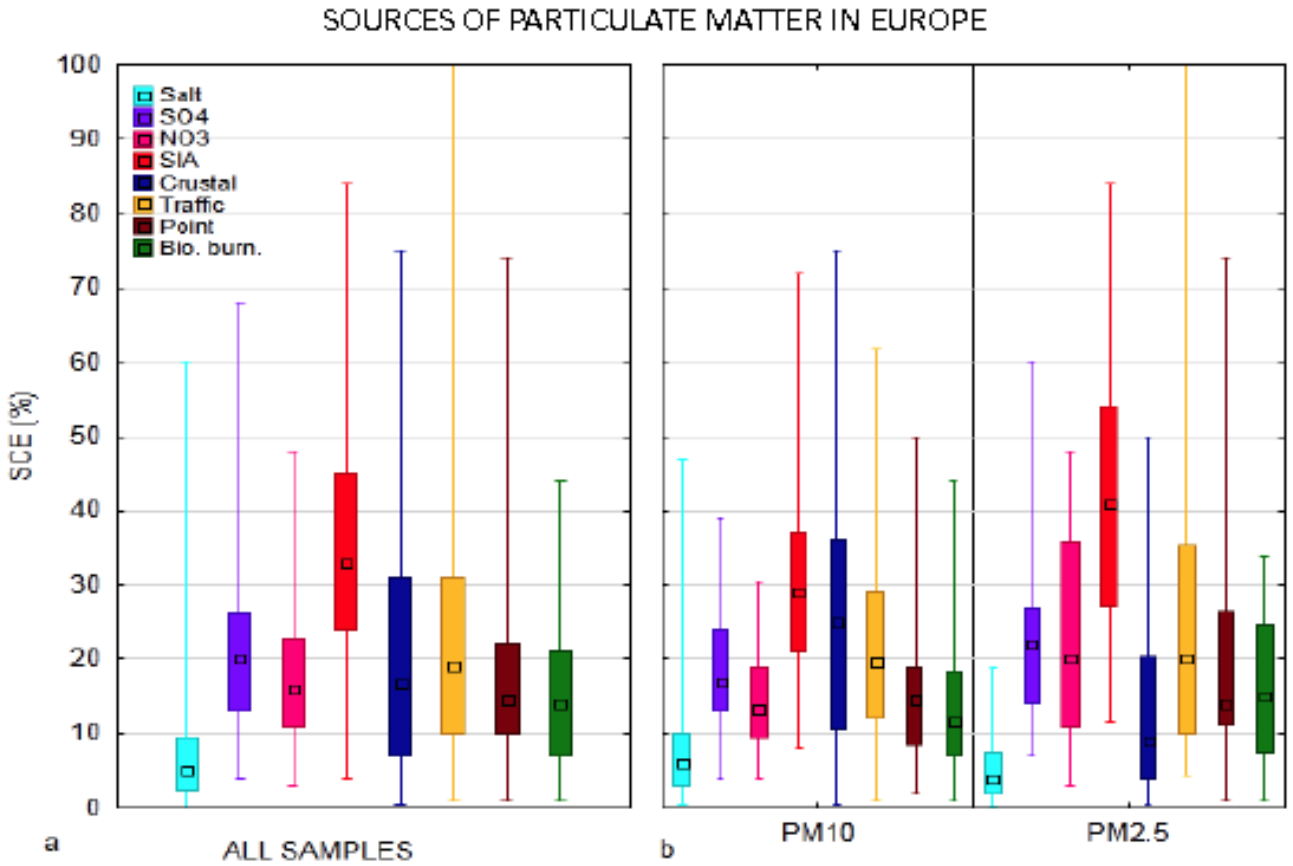

Six cathegories of sources in Europe

salt
sulphate } SIA
nitrate
crustal
traffic
point
bio. burn

Additional source coal combustion in specific areas

Source Contributions estimated with receptor models using measured PM_{10} and $PM_{2.5}$ chemical composition. 108 studies until 2012 - 272 records

Marker Median ± 25P-75P (box) ± Min-Max (whiskers)

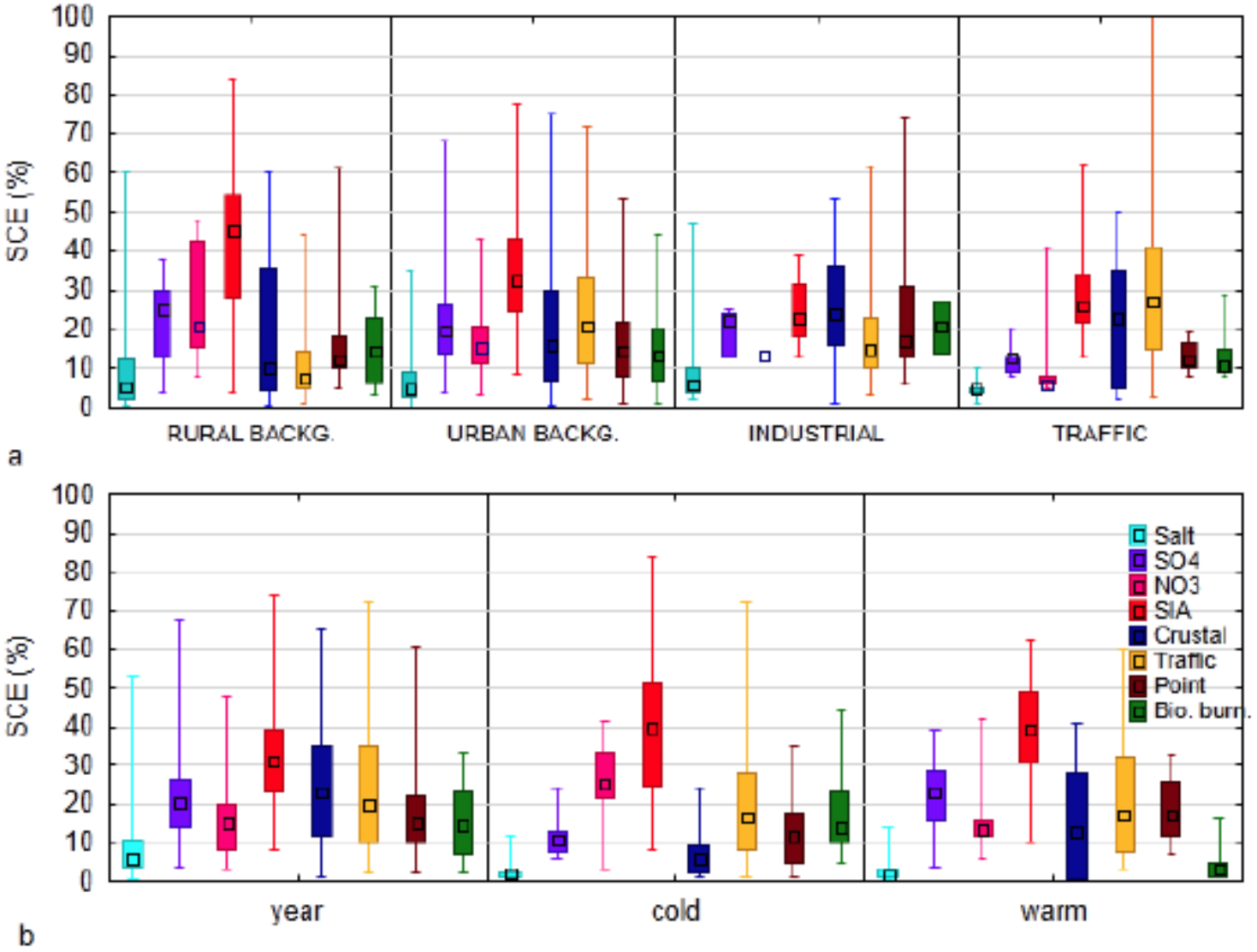

Differences between sites and seasonal trends

Critical review and meta-analysis of ambient particulate matter source apportionment using receptor models in Europe

C.A. Belis [a,*], F. Karagulian [a], B.R. Larsen [b], P.K. Hopke [c]

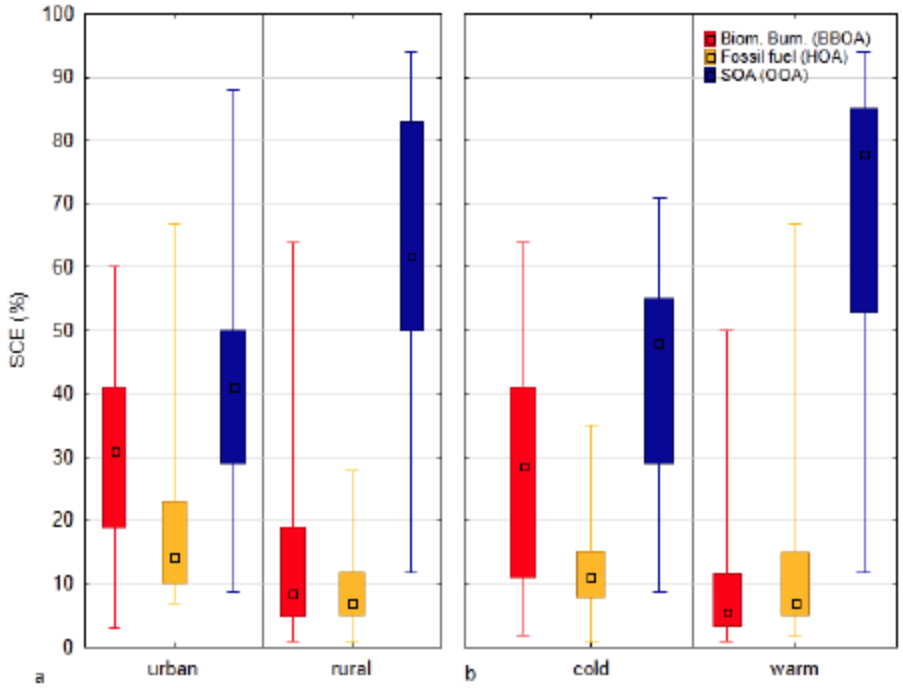

For the organic carbon (OC) fraction three main source categories were identified

Belis et al., 2016

Sources Profiles

1. Vehicular Emissions
2. Soil resuspension

TUNNEL JANIO QUADROS

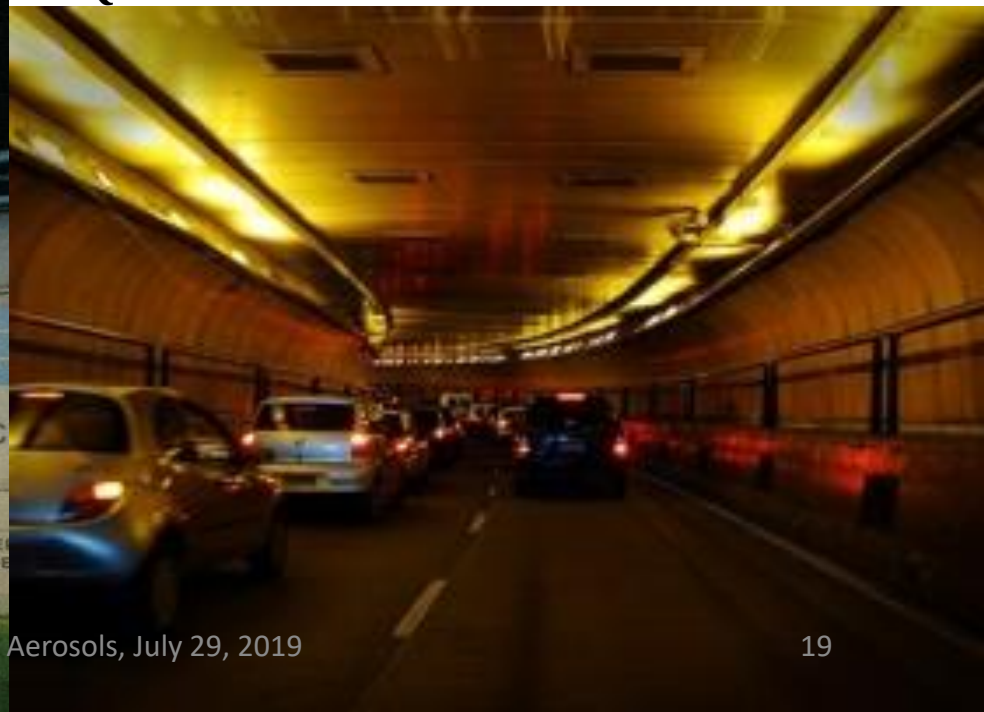

Traffic volume, proportion **heavy-duty vehicles** (p HDVs) & **pollutant** concentrations as function time day (TRA). **Emission factors** (EFs) NO_X vs. p HDVs

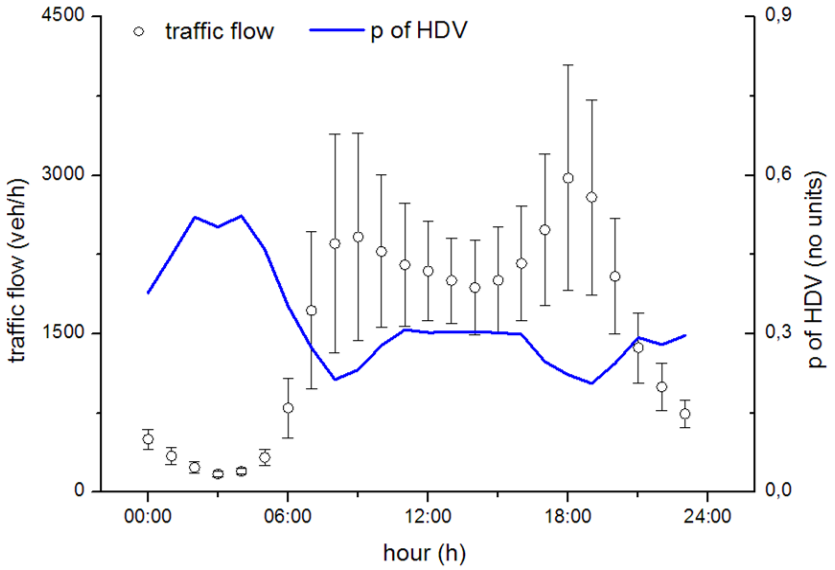

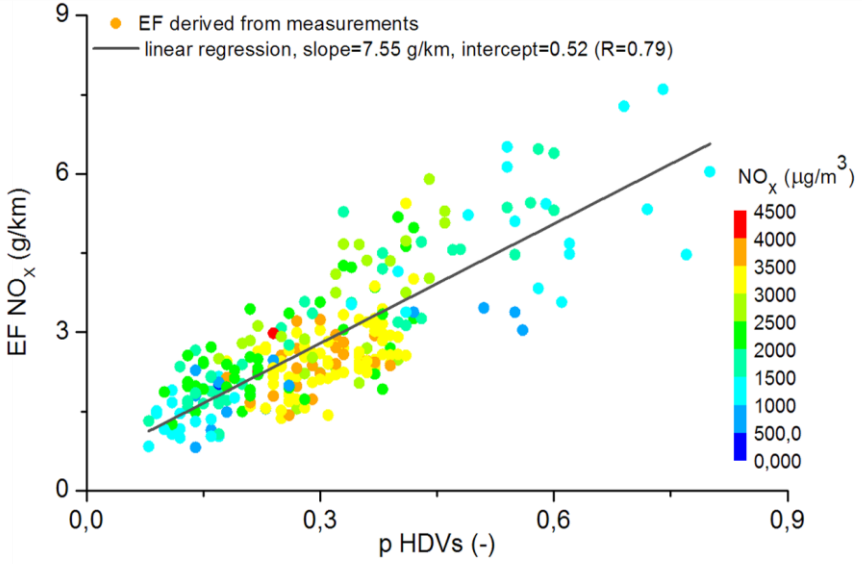

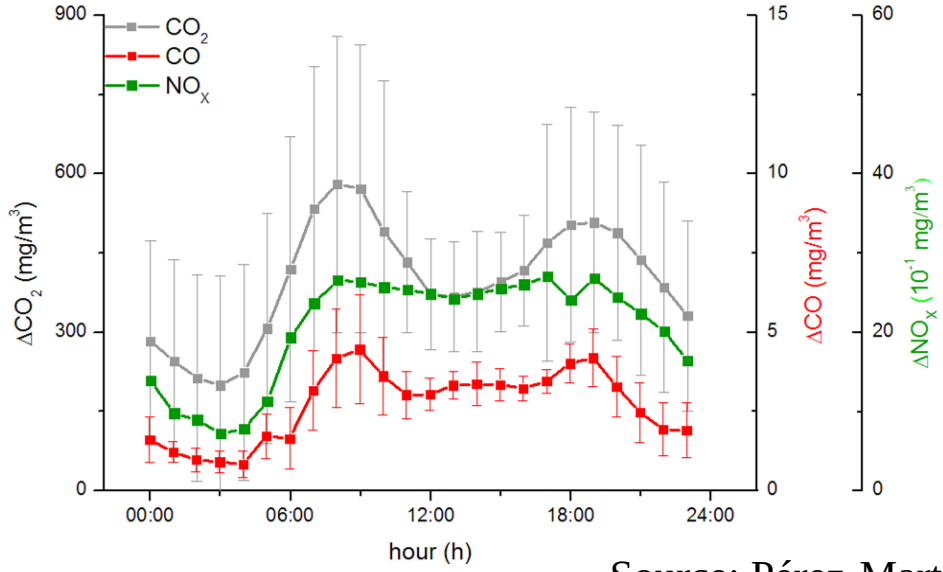

Veh.	Fuel (km kg^{-1})	CO (g km^{-1}) (g kg^{-1})	NO_x (g km^{-1}) (g kg^{-1})
LDV	13.7±18.4	5.8±3.8 81.5±41.5	0.3±0.2 4.2±1.7
HDV	2.23±2.71	3.6±1.5 7.9±4.1	9.2±2.7 25.8±7.6

Emissions SPMR (HC, CO, NO_x, MP, SO_x) ≈ **805 t/day** (88%, traffic)

Source: Pérez-Martínez et al. (2013)

Emission factors (g km^{-1}, g/kg of fuel burned) from 2011 in comparison with values calculated in 2004 study
(mean ± standard deviation).

Veh.	**Local measured**	**Fuel** (km kg^{-1})	**CO** (g km^{-1}) (g kg^{-1})	**NO_x** (g km^{-1}) (g kg^{-1})	**PM_{10}** (g km^{-1}) (µg kg^{-1})	**CO_2** (g km^{-1}) (g kg^{-1})
LDV	TJQ (2011)	13.7±18.4	5.8±3.8 78.9±25.3	0.3±0.2 4.2±2.6	0.178±0.143 2,441±44	219±165 3,001±85
HDV	TRA (2011)	2.24±2.71	3.5±1.5 7.8±4.3	9.2±2.7 25.5±8.1	0.290±0.248 692±663	1,427±1,178 3,177±90
LDV	TJQ (2004)[12]	n.d.	14.6±2.3 n.d.	1.6±0.3 n.d.	n.d. n.d.	n.d. n.d.
HDV	TMM[1] (2004) [12]	n.d.	20.6±4.7 n.d.	22.3±9.8 n.d.	n.d. n.d.	n.d. n.d.

Notes: [1]Tunnel María Maluf, São Paulo (2004).

Perez et al., 2013

Road Dust Emission

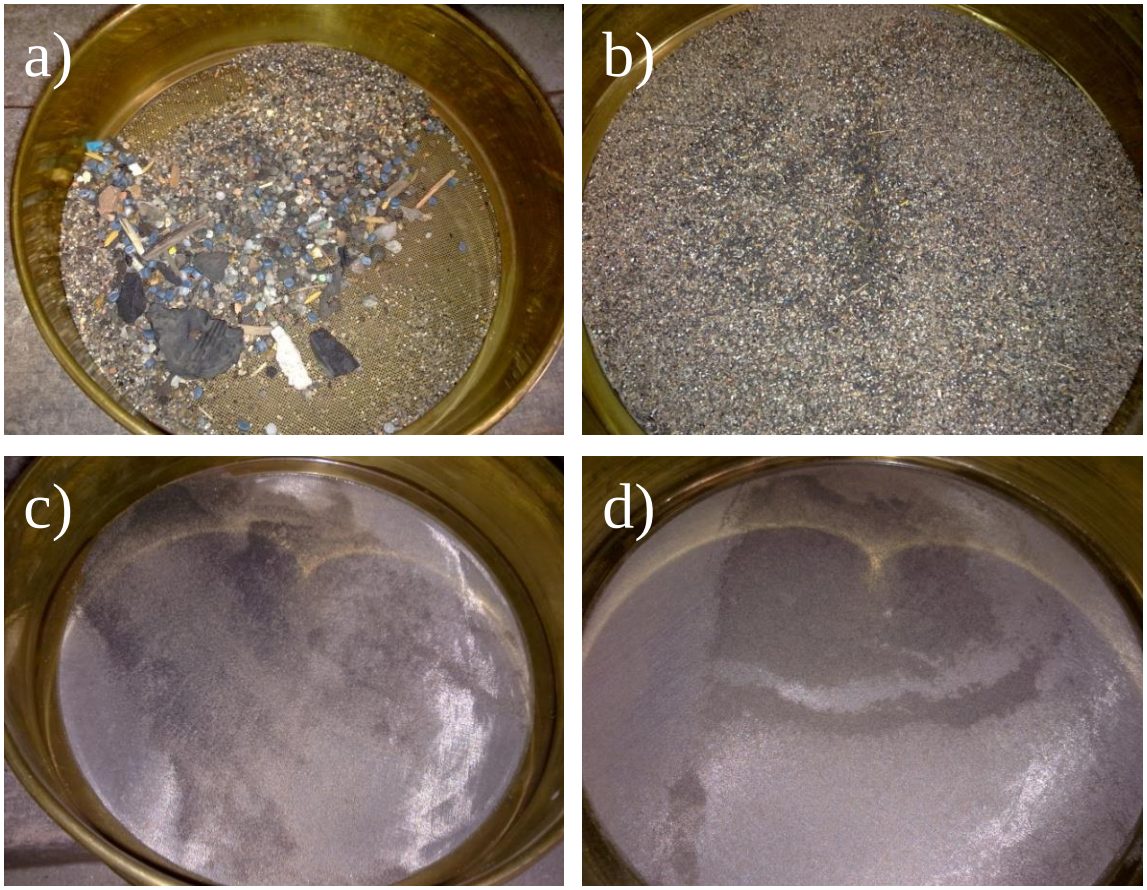

Hetem & Andrade, 2016

Table 2. Composition of the road dust as a percentage of the total mass of the resuspended material collected on the Teflon filters in the resuspension chamber.

Compound	IAG	RA_i	RA_o	JQ_i	JQ_o
BCe	1.96 ± 0.39	10.75 ± 4.3	1.52 ± 0.17	3.99 ± 1.99	1.04 ± 0.19
Al_2O_3	32.22 ± 6.44	19.27 ± 7.71	32.57 ± 3.58	13.99 ± 7	32.76 ± 5.9
SiO_2	33.41 ± 6.68	12.53 ± 5.01	30.68 ± 3.37	19.52 ± 9.76	29.36 ± 5.29
Fe_2O_3	4.54 ± 0.91	3.76 ± 1.5	6.18 ± 0.68	9.74 ± 4.87	4.75 ± 0.85
K_2O	2.15 ± 0.43	1.41 ± 0.56	1.78 ± 0.2	1.55 ± 0.78	1.32 ± 0.24
$CaCO_3$	2.85 ± 0.57	6.27 ± 2.51	3.98 ± 0.44	8.78 ± 4.39	7.77 ± 1.4
MgO	2.34 ± 0.47	1.11 ± 0.44	2.23 ± 0.24	1.97 ± 0.98	2.29 ± 0.41
$(NH_4)_2SO_4$	1.68 ± 0.34	10.99 ± 4.4	1.51 ± 0.17	6.77 ± 3.39	1.14 ± 0.21
Na	0.34 ± 0.07	0.73 ± 0.29	0.27 ± 0.03	0.7 ± 0.35	0.2 ± 0.04
TiO	0.61 ± 0.12	0.23 ± 0.09	0.57 ± 0.06	0.43 ± 0.22	0.65 ± 0.12
ZnO	0.11 ± 0.02	0.44 ± 0.18	0.2 ± 0.02	0.73 ± 0.36	0.13 ± 0.02
MnO_2	0.07 ± 0.01	0.11 ± 0.05	0.12 ± 0.01	0.16 ± 0.08	0.06 ± 0.01
P	0.06 ± 0.01	0.26 ± 0.11	0.44 ± 0.05	0.14 ± 0.07	0.04 ± 0.01
Cl	0.06 ± 0.01	0.74 ± 0.3	0.19 ± 0.02	0.53 ± 0.27	0.02 ± 0.004
CuO	0.04 ± 0.01	0.23 ± 0.09	0.06 ± 0.01	0.28 ± 0.14	0.05 ± 0.01
V_2O_5	0.01 ± 0.002	--	0.02 ± 0.002	0.02 ± 0.011	0.01 ± 0.002
Cr	--	--	0.05 ± 0.005	0.04 ± 0.018	0.03 ± 0.005
NiO	0.01 ± 0.002	0.04 ± 0.016	0.03 ± 0.004	0.01 ± 0.006	0.02 ± 0.003
Rb	0.01 ± 0.002	--	0.01 ± 0.001	0.004 ± 0.002	0.01 ± 0.001
Sr	0.02 ± 0.004	0.02 ± 0.007	0.03 ± 0.004	0.06 ± 0.032	0.02 ± 0.004
Cd	0.01 ± 0.001	--	0.01 ± 0.001	0.02 ± 0.011	0.01 ± 0.001
Sb	0.01 ± 0.003	0.08 ± 0.033	0.01 ± 0.001	0.1 ± 0.048	0.02 ± 0.004
Pb	0.03 ± 0.005	0.07 ± 0.028	0.01 ± 0.001	0.05 ± 0.026	0.01 ± 0.002
As	0.001 ± 0.0002	0.01 ± 0.0041	0.002 ± 0.0003	0.009 ± 0.0047	0.0004 ± 0.0001
Se	0.002 ± 0.0005	0.03 ± 0.01	--	0.01 ± 0.01	0.003 ± 0.001
Br	0.001 ± 0.0003	0.005 ± 0.0021	0.001 ± 0.0001	0.005 ± 0.0027	0.002 ± 0.0003

Values are expressed as average ± standard deviation. JQ_i and JQ_o, respectively, inside and outside the Jânio Quadros Tunnel (traveled primarily by light-duty and small, diesel-powered utility vehicles); RA_i and RA_o, respectively, inside and outside the Rodoanel Tunnel (traveled by a significant number of heavy-duty vehicles); and IAG, Institute of Astronomy, Geophysics, and Atmospheric Sciences (local street traveled by a mix of light- and heavy-duty vehicles).

Table 4. Profile of resuspended road dust from the three outside-tunnel sites evaluated in Brazil, together with comparable profiles for cities in Texas and for the city of Seville, Spain.

	Urban resuspended road dust profiles		
	Brazil	United States	Spain
Compound/element	% of total $PM_{2.5}$	% of total $PM_{2.5}$	% of total $PM_{2.5}$
BCe	1.50 ± 0.16	2.54 ± 0.28	5.3 ± 2.1
Si	10.37 ± 1.72	19.13 ± 2.10	-- ± --
Al	8.61 ± 1.42	6.81 ± 0.75	2.1 ± 0.6
Fe	5.15 ± 0.82	2.63 ± 0.29	2.5 ± 0.5
Ca	2.81 ± 0.47	30.11 ± 3.30	11.2 ± 3.1
Mg	1.38 ± 0.23	0.54 ± 0.06	1.9 ± 1.3
K	1.32 ± 0.22	1.42 ± 0.16	0.7 ± 0.2
Ti	0.61 ± 0.10	0.31 ± 0.03	1.6 ± 0.3
S	0.35 ± 0.06	3.04 ± 0.33	0.4 ± 0.1
Na	0.27 ± 0.04	0.02 ± 0.002	0.3 ± 0.1
P	0.18 ± 0.02	0.28 ± 0.03	0.1 ± 0.0
Zn	0.14 ± 0.02	0.22 ± 0.02	1.3 ± 0.3
Mn	0.07 ± 0.01	0.05 ± 0.01	0.37 ± 0.13
Cu	0.04 ± 0.01	0.03 ± 0.003	0.77 ± 0.27
Cl	0.04 ± 0.005	0.15 ± 0.02	0.9 ± 1.5
Cr	0.03 ± 0.002	0.02 ± 0.002	0.145 ± 0.061
Sr	0.0254 ± 0.0040	0.1537 ± 0.0169	-- ± --
Pb	0.0158 ± 0.0027	-- ± --	-- ± --
Sb	0.0118 ± 0.0020	-- ± --	-- ± --
Ni	0.0113 ± 0.0016	0.0090 ± 0.0010	-- ± --
V	0.01 ± 0.001	0.02 ± 0.002	0.0057 ± 0.001

Values are expressed as average ± standard deviation. Data for the United States (five sites within the cities of San Antonio and Laredo, Texas) were obtained from the SPECIATE 4.0 emissions profile database of the United States Environmental Protection Agency. Data for Spain (an urban site in the city of Seville) were obtained from Amato et al. [27].

Table 2.3 Marker Elements Associated with Various Emission Sources

Emission Source	Marker Elements*
Soil	Al, Si, Sc, Ti, Fe, Sm, Ca
Road dust	Ca, Al, Sc, Si, Ti, Fe, Sm
Sea salt	Na, Cl, Na^+, Cl^-, Br, I, Mg, Mg^{2+}
Oil burning	V, Ni, Mn, Fe, Cr, As, S, SO_4^{2-}
Coal burning	Al, Sc, Se, Co, As, Ti, Th, S
Iron and steel industries	Mn, Cr, Fe, Zn, W, Rb
Non-ferrous metal industries	Zn, Cu, As, Sb, Pb, Al
Glass industry	Sb, As, Pb
Cement industry	Ca
Refuse incineration	K, Zn, Pb, Sb
Biomass burning	K, C_{elem}, C_{org}, Br, Zn
Automobile gasoline	C_{elem}, Br, Ce, La, Pt, SO_4^{2-}, NO_3^-
Automobile diesel	C_{org}, C_{elem}, S, SO_4^{2-}, NO_3^-
Secondary aerosols	SO_4^{2-}, NO_3^-, NH_4^+

Table 3.2 Elements Measured in Chemical Analysis and Possible Sources

Elements	Possible Sources
Al, Si, Ca, Ti, Mn	Soils, Dust
S	Fossil fuels, Anthropogenic, and Biomass burning, Oceans, Soil Erosion
Cl	CFC's, Soil, Sea salt and Anthropogenic sources
K	Coal combustion, Biomass burning, Biomass fuels
V	Fuel oil and Steel factories
Cr	Emissions from Chemical plants, Cement dust and Crustal sources
Fe	Soils, Smelting industry
Ni	Heavy fuel oil combustion
Cu	Industries and Waste treatment
Zn	Combustion of coal and heavy fuel oil
As	Solid mineral fuels, Heavy fuel oil, Volcanoes, Smelting industry
Se	Heavy fuel oil and Glass production
Br	Gasoline, Transportation industry
Rb	Crustal sources
Pb	Paint industry, Leaded fuel use (banned)

Table 3.3 Typical Elemental, Ionic, and Carbon Source Markers

Source Type	Dominant Particle Size	Particle Abundance in Percent Mass			
		< 0.1%	0.1 to 1%	1 to 10%	> 10%
Paved Road	Coarse (2.5 to 10 µm)	Cr, Sr, Pb, Zr	SO_4^{2-}, Na^+, K^+, P, S, Cl, Mn, Zn, Ba, Ti	EC, Al, K, Ca, Fe	OC, Si
Unpaved Road Dust	Coarse	NO_3^-, NH_4^+, P, Zn, Sr, Ba	SO_4^{2-}, Na^+, K^+, P, S, Cl, Mn, Ba, Ti	OC, Al, K, Ca, Fe	Si
Construction	Coarse	Cr, Mn, Zn, Sr; Ba	SO_4^{2-}, K^+, S, Ti	OC, Al, K, Ca, Fe	Si
Agriculture Soil	Coarse	NO_3^-, NH_4^+, Cr, Zn, Sr	SO_4^{2-}, Na^+, K^+, S, Cl, Mn, Ba, Ti	OC, Al, K, Ca, Fe	Si
Natural Soil	Coarse	Cr, Mn, Sr, Zn, Ba	Cl^-, Na^+, EC, P, S, Cl, Ti	OC, Al, Mg, K, Ca, Fe	Si
Lake Bed	Coarse	Mn, Sr, Ba	K^+, Ti	SO_4^{2-}, Na^+, OC, Al, S, Cl, K, Ca, Fe	Si
Motor Vehicle'83-205	Fine (0 to 2.5 µm)	Cr, Ni, Y, Sr, Ba	Si, Cl, Al, Si, P, Ca, Mn, Fe, Zn, Br, Pb	Cl , NO_3^-, SO_4^{2-}, NH_4^+, S	OC, EC
Vegetative Burning	Fine	Ca, Mn, Fe, Zn, Br, Rb, Pb	NO_3^-, SO_4^{2-}, NH_4^+, Na+, S	Cl−, K^+, Cl, K	OC, EC
Residual Oil Combustion	Fine	K+, OC, Cl, Ti, Cr, Co, Ga, Se	NH_4^+, Na', Zn, Fe, Si	V, OC, EC, Ni	S, SO4'
Incinerator	Fine	V, Mn, Cu, Ag, Sn	K', Al, Ti, Zn, Hg ,	NO_3^-, Na^+, EC, Si, S, Ca, Fe, Br, La, Pb	SO_4^{2-}, NH_4^+, OC Cl
Coal-Fired Boiler	Fine	Cl, Cr, Mn, Ga, As, Se, Br, Rb, Zr	NH_4^+, P K, Ti, V, Ni, Zn, Sr, Ba, Pb	SO_4^{2-}, OC, EC, Al, S, Ca, Fe	Si
Oil Fired Power Plant	Fine	V, Ni, Se, As, Br, Ba	Al, Si, P, K, Zn	NH_4^+, OC, EC, Na, Ca, Pb	S, SO_4^{2-}
Smelters	Fine	V, Mn, Sb, Cr, Ti	Cd, Zn, Mg, Na, Ca, K, Se	Fe, Cu, As, Pb	S
Marine	Fine and Coarse	Ti, V, Ni, Sr, Zr, Pd, Ag, Sn, Sb, Pb	Al, Si, K, Ca, Fe, Cu, Zn, Ba, La	NO_3^-, SO_4^{2-}, OC, EC	Cl^-, Na^+, Na, Cl

Source: Chow, 1995.

Figure A3.1 Commonly Measured Elements, Ion, and Organic Markers

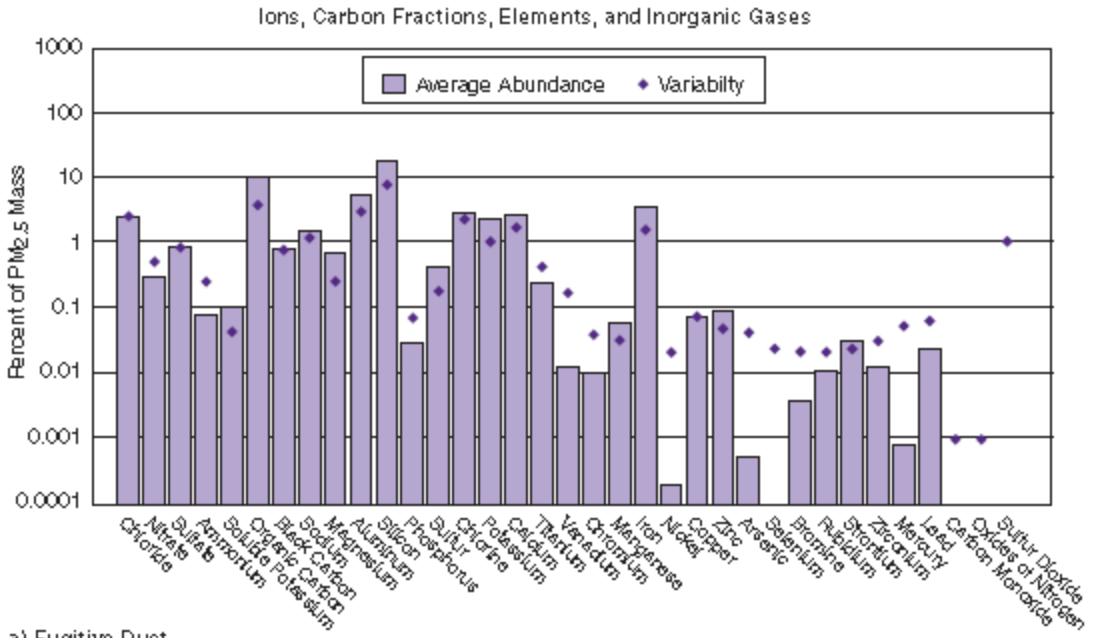

a) Fugitive Dust

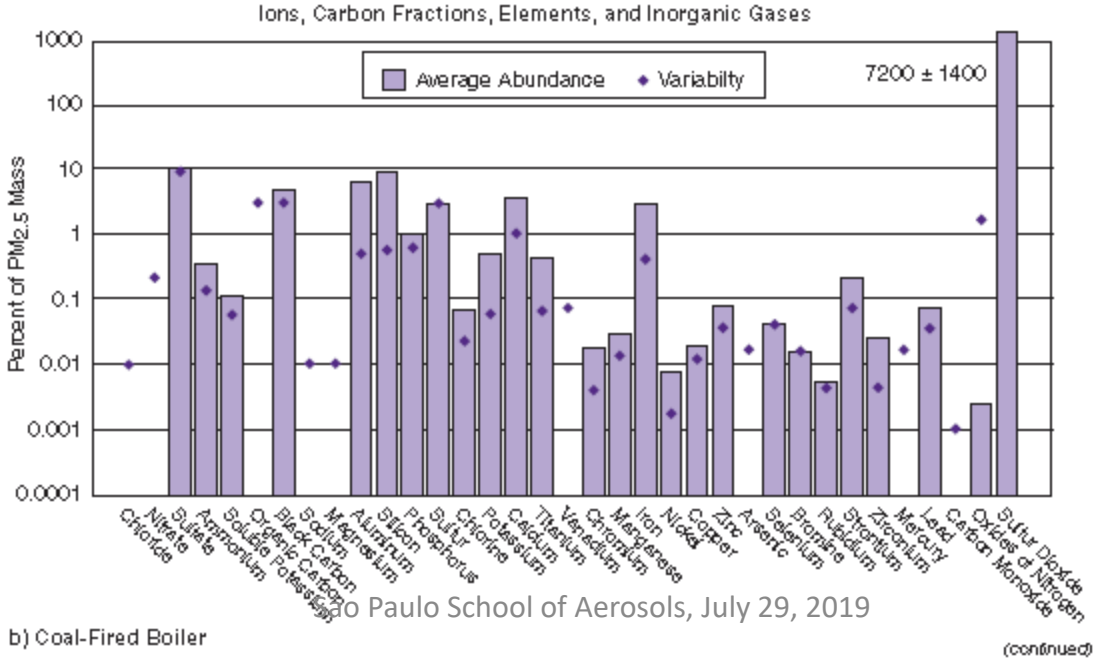

b) Coal-Fired Boiler

(continued)

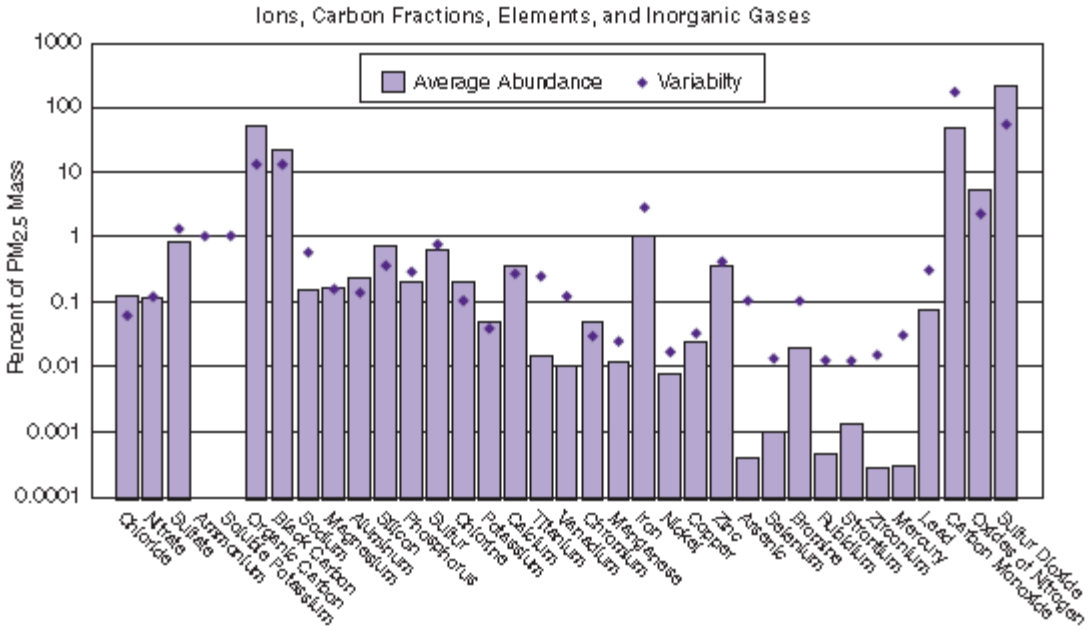

c) Gas Veh. Exhaust

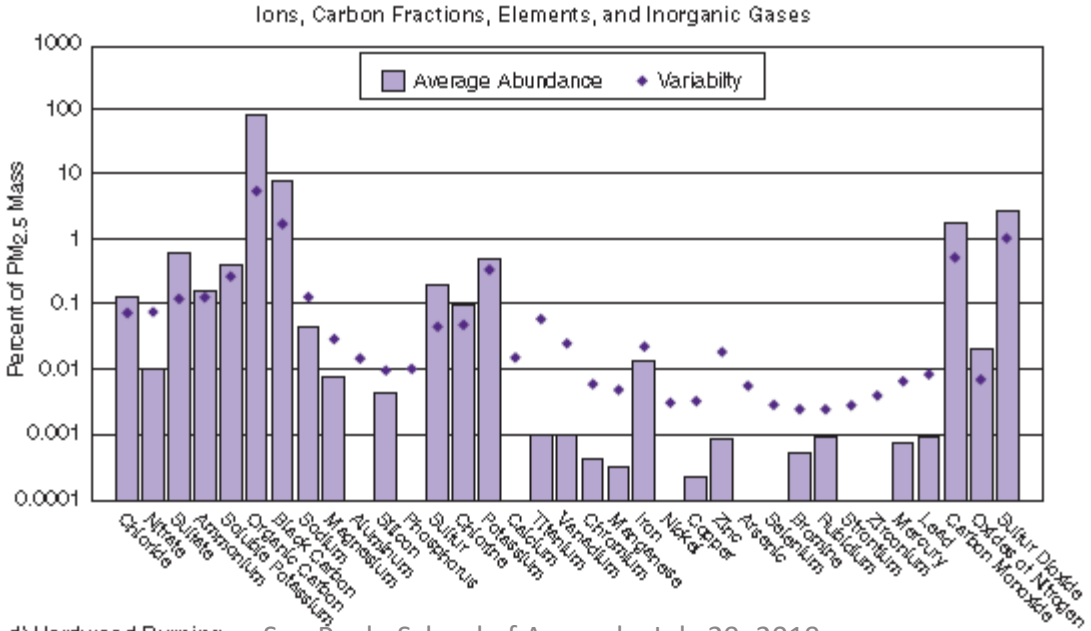

d) Hardwood Burning

Examples in São Paulo

CMB Receptor Models

CETESB, 2002

RUA: poeira de rua coletada em Cerqueira César, nas imediações da estação de amostragem;
VEIC: emissão veicular;
SULSEC: sulfatos secundários;
CARSEC: carbono secundário;
NITSEC: nitratos secundários;
QUEIMA: fonte de combustão de resíduos;
COMBIO: fonte de combustão de biomassa;
CIMENTO: material particulado proveniente de cimento Portland;
MAR: fonte de aerossol marinho.

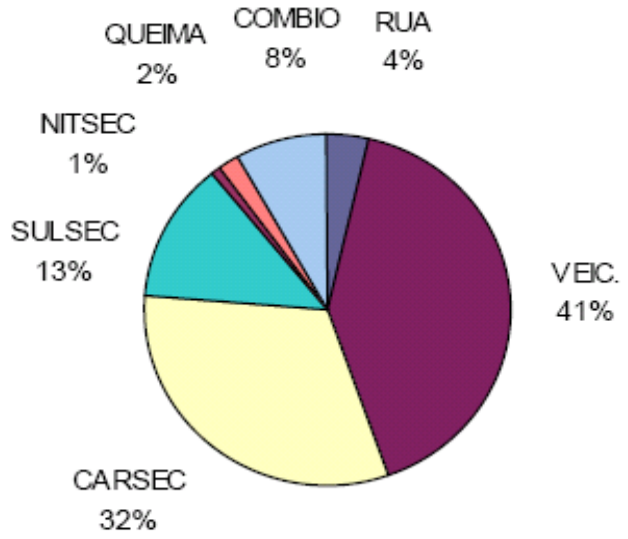

Source of PM2.5 in Cerqueira César in1993

Concentração média: 68 µg/m^3

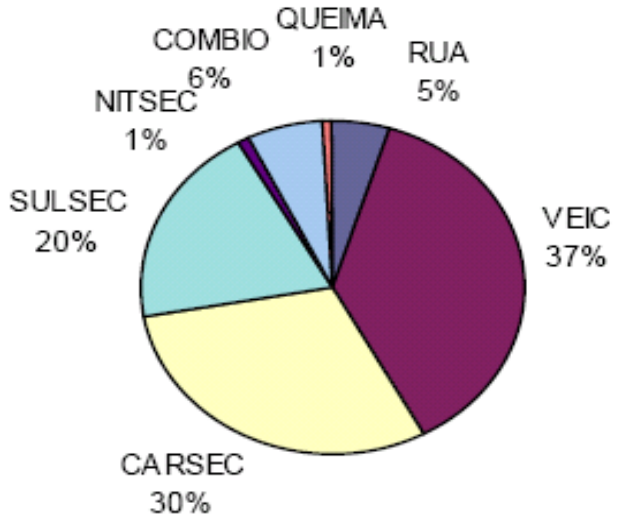

Sources in Cerqueira César in 1996/97.

Concentração média: 40 µg/m^3

(Cetesb, 2002)

II. Multivariate Analysis

Principal Component Analysis

-**Reduce the dimension of the data matrix using the relation of covariance among the variables.**

Principal Component Analysis

- Introduced by Pearson (1901) and Hotelling (1933) to describe the variation of a multivariate data set in terms of an uncorrelated set of variables.
- Matrix with n observation in p correlated $x_1, x_2, \ldots x_p$
- PCA seeks one transformation of x_i *in* p new variables y_i that are not correlated

PCA objectives

- Extract the true dimension of the data.
- That is, the dataset of dimension p can be represented by q<p dimensions without losing information.
- Interpretation of the main components (“new” variables).

$\mathbf{x}$ vector of p original variables $\mathbf{x}^T = (X_1, \ldots, X_p)$, with $Cov(\mathbf{x}) = \Sigma$. Consider p linear combinations for $X_1, \ldots, X_p$

$$Y_1 = \boldsymbol{l}_1^T\mathbf{x} = l_{11}X_1 + l_{12}X_2 + \ldots + l_{1p}X_p$$

$$Y_2 = \boldsymbol{l}_2^T\mathbf{x} = l_{21}X_1 + l_{22}X_2 + \ldots + l_{2p}X_p$$

$$\vdots$$

$$Y_p = \boldsymbol{l}_p^T\mathbf{x} = l_{p1}X_1 + l_{p2}X_2 + \ldots + l_{pp}X_p$$

So $Var(Y_i) = \boldsymbol{l}_i^T\, Var(\mathbf{x})\, \boldsymbol{l}_i = \boldsymbol{l}_i^T\, \Sigma\, \boldsymbol{l}_i$ e $Cov(Y_i, Y_j) = Cov(\boldsymbol{l}_i^T\mathbf{x}, \boldsymbol{l}_j^T\mathbf{x}) = \boldsymbol{l}_i^T\Sigma\boldsymbol{l}_j$. The Principal Components are the linear combinations

$Y_1, \ldots, Y_p$ not correlated, with the highest possible variances.

Como Obter as Componentes Principais

The i-ésima Principal Component is the linear combination

$\boldsymbol{l}_i^T\mathbf{x}$

That maximize

$\text{Var}(\boldsymbol{l}_i^T\mathbf{x})$

With the characteristics

$\boldsymbol{l}_i^T\boldsymbol{l}_i = 1 \quad \text{Cov}(\boldsymbol{l}_i^T\mathbf{x}, \boldsymbol{l}_j^T\mathbf{x}) = 0,$

To any j < i. These restrictions ensure that the sum of the variances of the original variables is equal to the sum of the variances of the principal components and that they are uncorrelated.

How to obtain the Principal Components

Be Σ the covariance matrix associated with the random variable vector $\mathbf{x}$. Be $(\lambda_1, \boldsymbol{\alpha}_1), \ldots, (\lambda_p, \boldsymbol{\alpha}_p)$ eigenvalues and standard orthogonal eigenvectors associated with Σ, sorted so that $\lambda_1 \geq \lambda_2 \geq \ldots \geq \lambda_p \geq 0$. The *i*-ésima Principal componente is

$$Y_i = \alpha_i^T \mathbf{x} = \alpha_{i1}X_1 + \alpha_{i2}X_2 + \ldots + \alpha_{ip}X_p,$$

i = 1, 2, . . ., p. With

$$Var(Y_i) = \alpha_i^T \Sigma \alpha_i = \lambda_i \text{ , } i = 1, 2, \ldots, p$$

$$Cov(Y_i, Y_j) = \alpha_i^T \Sigma \alpha_j = 0, \; i \neq j$$

The magnitude of αij measures the importance of the jth variable for the ith principal component.

Properties of PC

- It is important to note how much of the total variability is explained by each major component. To find this measure, simply calculate;

$$\frac{\lambda_i}{\lambda_1 + \lambda_2 + \ldots + \lambda_p}, i = 1, 2, \ldots, p;$$

- Principal Components can also be obtained from standard variables, ie from the correlation matrix;
- The principal components derived from the covariance matrix Σ are generally different from the principal components derived from the correlation matrix ρ;
- If the data follow a Multivariate Normal distribution, the eigenvalues of Σ are distinct and the principal component analysis is based on the Maximum Likelihood Estimator of the covariance matrix.

MP2.5 composition

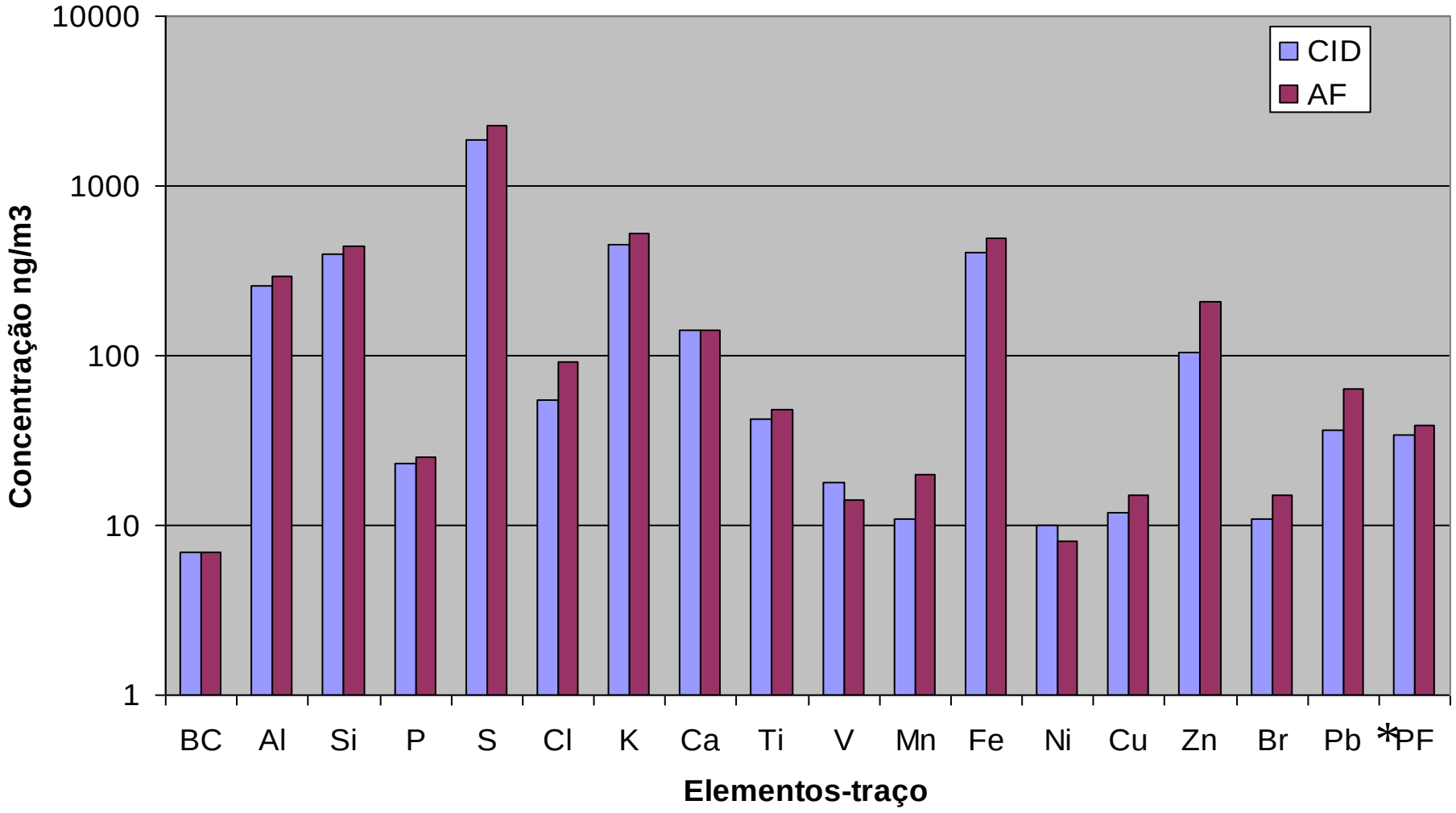

*BC e FP in µg/m3

Receptor Models ACP MP2.5 São Paulo

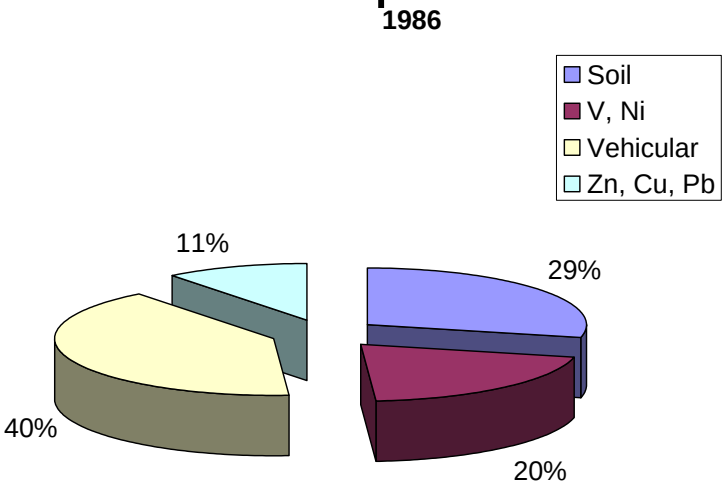

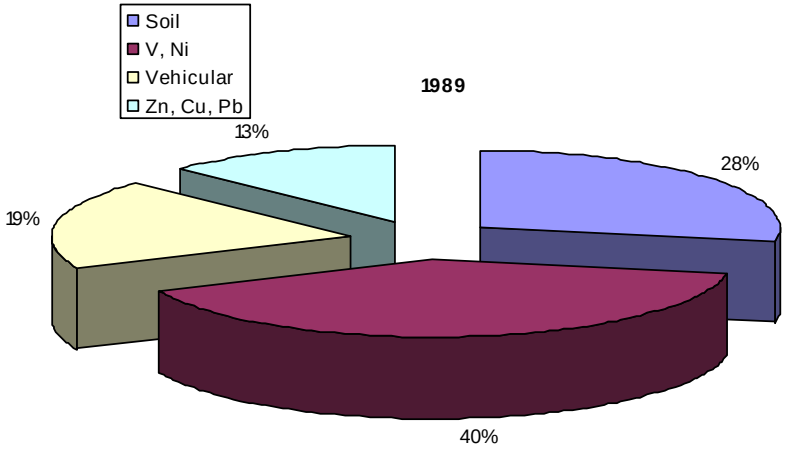

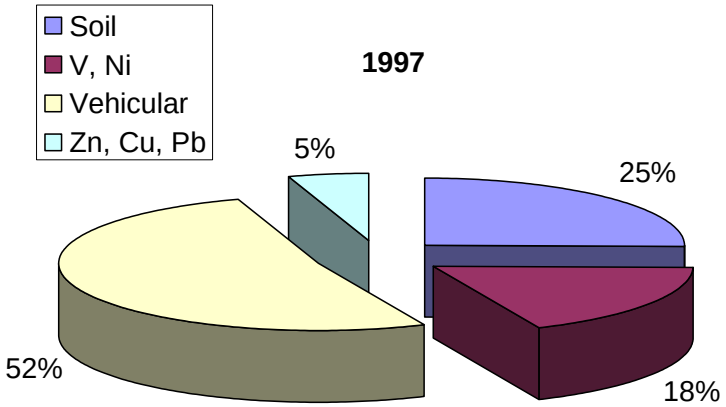

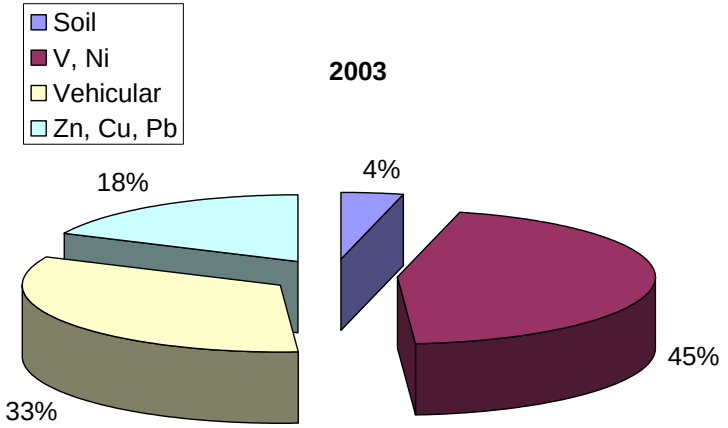

Wintertime and summertime São Paulo aerosol source apportionment study

Andréa D.A. Castanho*, Paulo Artaxo

Atmospheric Environment 35 (2001) 4889–4902

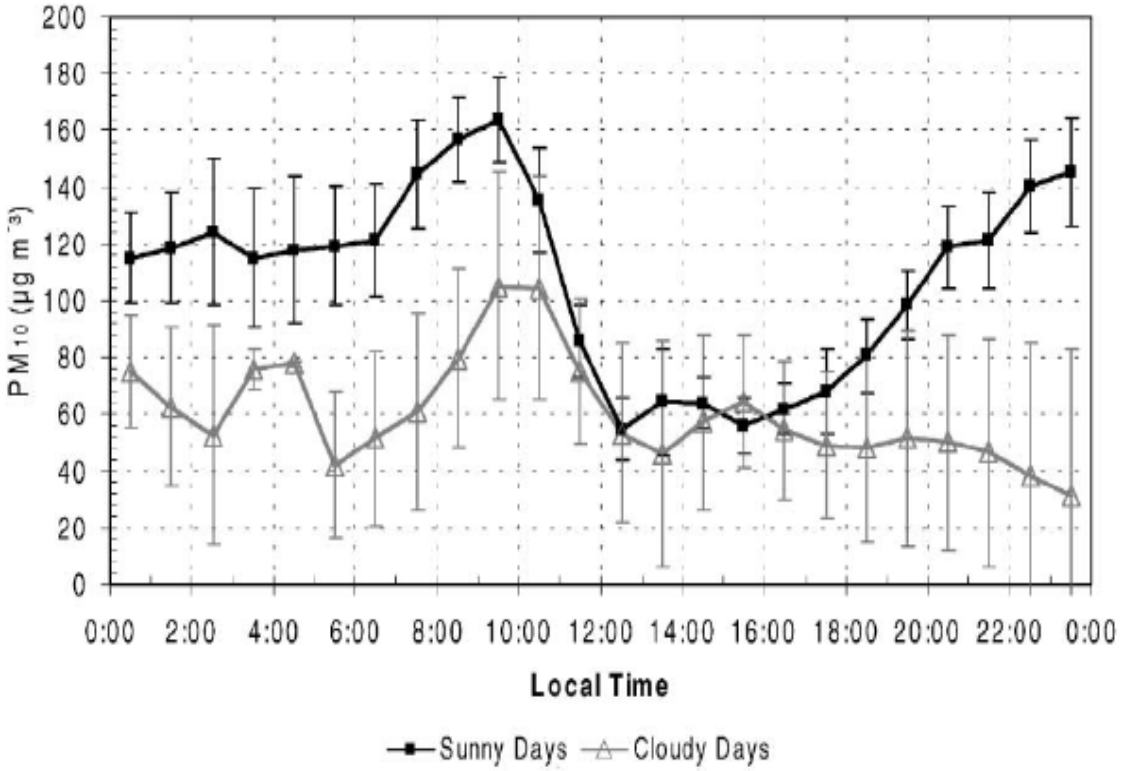

Fig. 3. Average diurnal cycle of PM_{10} concentrations during weekdays. The plot presents 1-h average of sunny (8 days) and cloudy (3 days) weekdays measured in wintertime from 10 July to 10 September in 1997 in São Paulo by the TEOM PM_{10} monitor.

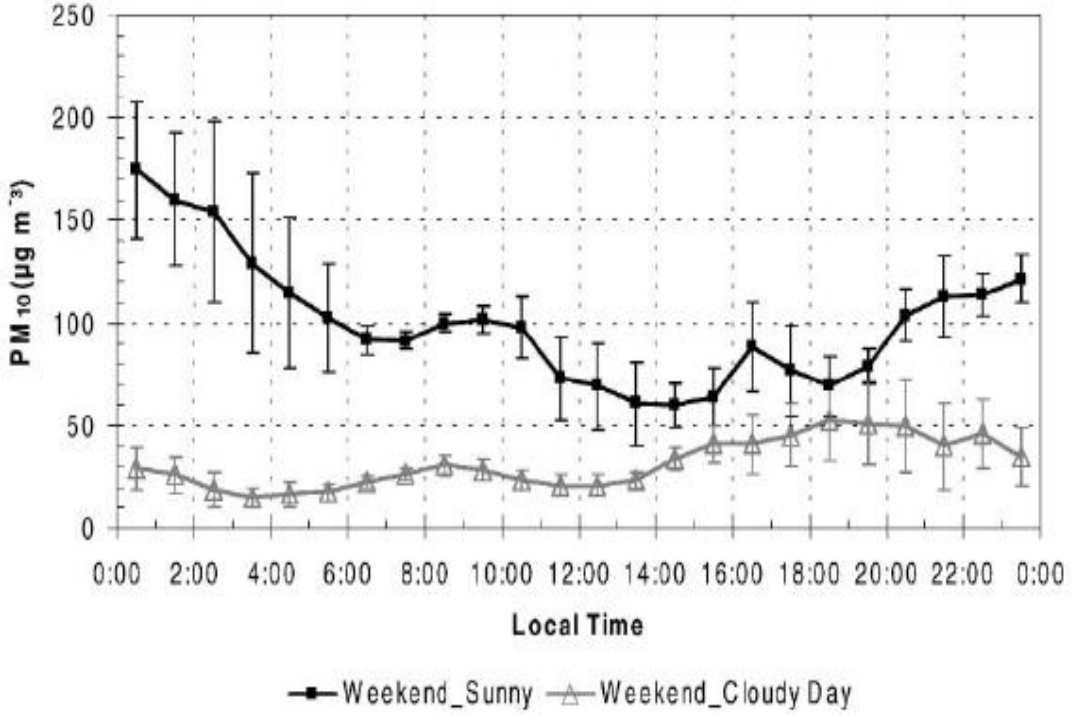

Fig. 4. Diurnal cycle of mass concentration of PM_{10} on weekend's days. The figure shows 1-h average of sunny (4 days) and cloudy (4 days) days data measured in wintertime from 10 July to 10 September in 1997 in São Paulo by the TEOM PM_{10} monitor.

Castanho & Artaxo, 2001

Table 1
Descriptive statistics of the fine and coarse mode particulate matter during the wintertime sampling period, from 10 July to 10 September in 1997 in the São Paulo metropolitan area

$PM_{2.5}$ aerosol ($d_p < 2.5\,\mu m$)				Coarse mode aerosol ($2.5 < d_p < 10\,\mu m$)			
Specie	Mean ($ng\,m^{-3}$)	σ[a] ($ng\,m^{-3}$)	Number of samples	Specie	Mean ($ng\,m^{-3}$)	σ ($ng\,m^{-3}$)	Number of samples
$PM_{2.5}$[b]	30.2[b]	16.1[b]	181	CPM[b]	46.1[b]	38.1[b]	177
Black carbon[b]	7.6[b]	3.7[b]	181	—	—	—	—
Organic carbon[b]	15.8[b]	8.3[b]	57	—	—	—	—
Al	437	282	179	Al	1521	1212	177
Si	511	288	179	Si	2269	1726	177
P	14.3	4.9	25	P	25	14	114
S	1510	1166	179	S	733	580	177
Cl	52	35	78	Cl	250	279	177
K	407	252	179	K	486	433	177
Ca	146	93	179	Ca	1196	864	177
Ti	31	24	179	Ti	217	165	177
V	11.7	6.5	179	V	12	12	177
Cr	9.6	3.7	9	Cr	24	15	51
Mn	12.6	8.1	179	Mn	32	23	177
Fe	532	273	179	Fe	1981	1426	177
Ni	3.9	2.8	179	Ni	5.8	6.2	177
Cu	19	11	179	Cu	44	44	177
Zn	126	107	179	Zn	189	234	177
Se	3.0	2.6	123	Se	3.0	3.4	86
Br	14.3	6.2	65	Br	24	14	27
Rb	4.6	2.5	84	Rb	7.6	4.9	106
Sr	2.4	1.0	72	Sr	8.5	6.2	177
Zr	4.1	2.1	28	Zr	12	15	101
Pb	42	34	179	Pb	38	45	177

[a] σ is the standard deviation of the concentration distribution.
[b] Concentrations in ($\mu g\,m^{-3}$).

Castanho & Artaxo, 2001

Table 3
VARIMAX rotated factor loading matrix for the elemental, $PM_{2.5}$ and black carbon concentrations of the fine particulate matter sampled in wintertime from 10 July to 10 September 1997 in São Paulo city[a]

Element	Factor 1	Factor 2	Factor 3	Factor 4	Factor 5	Factor 6	Communalities
	Soil dust 1	Motor vehicles	Sulfates	Oil combustion	Industry	Soil dust 2	
Al	0.94	0.11	0.12	—	—	—	0.92
Si	0.89	0.20	—	—	—	0.21	0.88
Ti	0.76	—	0.19	—		0.51	0.89
Cu	0.22	0.88	—	0.15	0.20	0.23	0.94
Bc	0.23	0.80	0.31	0.27	0.22	—	0.91
S	—	—	0.75	0.33	0.43	0.22	0.91
$PM_{2.5}$	0.24	0.47	0.70	0.28	0.29	0.21	0.97
K	0.43	0.29	0.68	0.33	—	0.15	0.87
V	—	0.29	0.29	0.86	0.16	—	0.94
Ni	—	0.18	0.25	0.81	0.43	—	0.93
Zn	—	0.35	0.22	0.33	0.80	—	0.92
Pb	—	0.56	0.36	0.35	0.60	—	0.93
Ca	0.58	0.12	0.17	—	—	0.67	0.83
Mn	0.23	0.17	0.33	0.27	0.55	0.58	0.90
Fe	0.52	0.45	0.23	0.21	0.16	0.56	0.91
Variance (%)	21.8	17.2	14.6	14.2	12.8	10.6	91.1

[a] Only factor loadings larger than 0.1 are shown.

Castanho & Artaxo, 2001

Table 5
Correlation coefficients between factor scores identified by the APFA procedure in wintertime and the concentrations of CO, NO_2 and SO_2 and organic carbon obtained by the carbon monitor in the same period[a]

Fine particulate sources	Gaseous species			Carbon monitor
	CO	NO_x	SO_2	Organic carbon
Soil dust 1	0.35	0.33	0.58	0.56
Motor vehicle	0.80	0.75	0.43	0.71
Sulfates	—	−0.24	—	−0.17
Oil combustion	—	—	—	—
Industry	—	—	—	—
Soil dust 2	—	—	0.35	—

[a] Only statistically significant (within 95% confidence interval) correlation coefficients are shown.

Castanho & Artaxo, 2001

Table 6
Absolute aerosol source apportionment for the elemental, $PM_{2.5}$ and black carbon concentrations of the fine particulate matter sampled in wintertime from 10 July to 10 September 1997 in São Paulo[a]

	Factor 1	Factor 2	Factor 3	Factor 4	Factor 5	Factor 6	Concentration
($ng\,m^{-3}$)	Soil dust 1	Vehicle traffic	Sulfates	Oil combustion	Industry	Soil dust 2	Model/measured
$PM_{2.5}$[b]	5.9	8.5	7.0	5.6	1.5	1.6	1.01
Bc[b]	1.5	3.4	0.75	1.4	0.27	—	1.03
Al	378	40.7	21.5	—	5.7	−6.4	0.99
Si	372	69	—	36.0	5.5	25.4	1.01
S	—	86	557	520	162	140	1.03
K	139	70	102	87	—	12.2	0.99
Ca	85	15.8	11.1	—	—	30.4	1.03
Ti	24.7	—	2.5	—	−0.92	5.5	0.98
V	0.80	2.2	1.2	6.8	0.34	0.23	1.01
Mn	3.0	1.6	1.7	2.6	1.4	2.3	1.00
Fe	207	131	38.8	66.8	14.2	73	1.00
Ni	−0.21	0.53	0.42	2.6	0.38	0.08	1.00
Cu	3.8	11.1	—	2.0	0.74	1.2	1.02
Zn	—	39.8	14.3	41.3	27.4	3.5	1.00
Pb	−2.7	19.6	7.1	13.1	6.5	−0.73	0.98

[a] $PM_{2.5}$: fine mode particulate matter; BC: black carbon.
[b] Concentration in ($\mu g\,m^{-3}$).

Castanho & Artaxo, 2001

Determination of source contributions of NMHCs in Helsinki (60°N, 25°E) using chemical mass balance and the Unmix multivariate receptor models

Heidi Hellén*, Hannele Hakola, Tuomas Laurila

Atmospheric Environment 37 (2003) 1413–1424

Table 1
Average concentrations (μg/m^3) in the ambient air during different seasons and the source profiles for NMHC emissions in Helsinki used in the CMB study

Species	Mar	Jun	Aug	Nov	LG	GVs	GVw	GE	DE	DSs	DSw	CG	B
Ethane*	4.22	2.31	2.40	3.55	0.00	0.00	0.01	0.02	0.04	0.20	0.24	0.54	
Ethene*	2.14	0.79	1.13	1.88	0.00	0.00	0.00	0.09	0.44	0.04	0.04	0.00	
Propane*	3.31	1.18	1.58	3.30	0.00	0.03	0.05	0.00	0.02	0.15	0.18	0.27	
Propene*	0.71	0.37	0.49	0.75	0.00	0.00	0.00	0.04	0.14	0.01	0.01	0.01	
2-Methylpropane*	1.66	0.80	0.88	1.78	0.01	0.08	0.08	0.01	0.01	0.04	0.05	0.07	
Ethyne*	2.28	0.77	0.81	1.77	0.00	0.00	0.00	0.06	0.10	0.05	0.04	0.00	
Butane*	5.45	2.32	2.73	4.86	0.11	0.44	0.58	0.06	0.02	0.07	0.11	0.07	
trans-2-Butene	0.04	0.10	0.10	0.13	0.00	0.02	0.02	0.00	0.01	0.00	0.00	0.00	
1-Butene*	0.20	0.13	0.15	0.17	0.00	0.01	0.01	0.01	0.03	0.00	0.00	0.00	
2-Methylpropene	0.55	0.30	0.83	0.42	0.00	0.01	0.00	0.02	0.02	0.02	0.01	0.00	
cis-2-Butene	0.14	0.05	0.09	0.11	0.00	0.02	0.01	0.00	0.01	0.00	0.00	0.00	
2-Methylbutane*	2.30	1.40	1.75	2.61	0.10	0.14	0.11	0.05	0.01	0.05	0.05	0.02	
Pentane*	1.12	0.77	0.97	1.55	0.04	0.08	0.03	0.02	0.01	0.04	0.04	0.01	
Propyne*	0.05	0.02	0.03	0.04	0.00	0.00	0.00	0.00	0.01	0.00	0.00	0.00	
1,3-Butadiene	0.18	0.09	0.13	0.16	0.00	0.00	0.00	0.01	0.03	0.00	0.00	0.00	
trans-2-Pentene	0.15	0.08	0.09	0.12	0.01	0.01	0.00	0.00	0.00	0.00	0.00	0.00	
cis-2-Pentene	0.06	0.05	0.06	0.06	0.00	0.00	0.00	0.00	0.00	0.00	0.00	0.00	
Cyclohexane*	0.29	0.15	0.32	0.42	0.01	0.01	0.00	0.01	0.00	0.02	0.01	0.00	
2-Methylpentane*	0.66	0.42	0.58	0.77	0.04	0.04	0.01	0.03	0.00	0.01	0.01	0.00	
3-Methylpentane*	0.41	0.27	0.39	0.48	0.04	0.02	0.01	0.02	0.00	0.01	0.01	0.00	
Hexane*	1.00	1.09	0.46	0.72	0.03	0.02	0.00	0.01	0.00	0.02	0.02	0.00	
Isoprene*	0.14	0.12	0.64	0.09	0.00	0.00	0.00	0.00	0.00	0.00	0.00	0.00	0.34
Heptane*	0.46	0.38	0.31	0.65	0.02	0.00	0.00	0.01	0.00	0.00	0.01	0.00	
Benzene**	1.85	0.68	1.04	1.24	0.02	0.01	0.00	0.04	0.03	0.09	0.06	0.00	
Toluene**	4.09	2.17	3.45	4.16	0.17	0.03	0.01	0.14	0.03	0.06	0.05	0.00	
MTBE**	1.99	1.68	2.15	2.15	0.06	0.00	0.05	0.04	0.00	0.04	0.01	0.00	
TAME**	0.53	0.34	0.42	0.61	0.06	0.01	0.01	0.04	0.00	0.01	0.00	0.00	
Ethylbenzene**	0.82	0.51	0.67	0.85	0.03	0.00	0.00	0.04	0.00	0.01	0.01	0.00	
p/m-Xylene**	2.42	1.49	1.87	2.43	0.07	0.01	0.00	0.09	0.01	0.02	0.02	0.00	
Styrene	0.06	<DL	0.05	<DL	0.00	0.00	0.00	0.01	0.00	0.01	0.00	0.00	
o-Xylene**	0.98	0.59	0.78	1.01	0.03	0.00	0.00	0.04	0.00	0.01	0.01	0.00	
α-Pinene**	0.09	0.19	0.41	0.09	0.00	0.00	0.00	0.00	0.00	0.00	0.00	0.00	0.34
Propylbenzene**	0.22	0.11	0.18	0.20	0.01	0.00	0.00	0.01	0.00	0.00	0.00	0.00	
3-Ethyltoluene**	0.55	0.29	0.44	0.53	0.02	0.00	0.00	0.02	0.00	0.00	0.00	0.00	
Camphene	<DL	<DL	0.02	0.03	0.00	0.00	0.00	0.00	0.00	0.00	0.00	0.00	0.04
4-Ethyltoluene**	0.26	0.14	0.22	0.24	0.01	0.00	0.00	0.01	0.00	0.00	0.00	0.00	
1,3,5-Trimethylbenzene	0.25	0.13	0.21	0.27	0.01	0.00	0.00	0.01	0.00	0.00	0.00	0.00	
Sabinene	n.d.	n.d.	0.01	n.d.	0.00	0.00	0.00	0.00	0.00	0.00	0.00	0.00	0.00
2-Ethyltoluene**	0.23	0.14	0.21	0.22	0.01	0.00	0.00	0.01	0.00	0.00	0.00	0.00	
β-Pinene**	0.02	0.04	0.10	0.03	0.00	0.00	0.00	0.00	0.00	0.00	0.00	0.00	0.09
1,2,4-Trimethylbenzene**	0.87	0.46	0.75	0.92	0.03	0.00	0.00	0.02	0.00	0.01	0.01	0.00	
3-Carene**	<DL	0.05	0.12	0.03	0.00	0.00	0.00	0.00	0.00	0.00	0.00	0.00	0.09
1,2,3-Trimethylbenzene**	0.23	0.13	0.24	0.25	0.01	0.00	0.00	0.01	0.00	0.00	0.00	0.00	
Limonene	<DL	<DL	<DL	<DL	0.00	0.00	0.00	0.00	0.00	0.00	0.00	0.00	0.04
1,8-Cineol	<DL	0.02	0.03	0.01	0.00	0.00	0.00	0.00	0.00	0.00	0.00	0.00	0.05

Note: LG = liquid gasoline, GVs = gasoline vapour in summer, GVw = gasoline vapour in winter, GE = gasoline exhaust, DE = diesel exhaust, DSs = distant sources in summer, DSw = distant sources in winter, CG = city gas, B = biogenic sources. Fitting species used in CMB only are marked with (*) and fitting species in CMB and in Unmix with (**).

Hellen, 2003

Table 2
Source contributions ± standard deviation (as % of measured mass) of NMHCs given by the CMB model using 24-h samples and measured source profiles

	March	June	August	November	Year 2001
Liquid gasoline	4.0 ± 3.1	13.0 ± 5.7	16.7 ± 5.9	16.0 ± 9.7	12.4 ± 5.9
Gasoline vapour	10.4 ± 2.3	9.5 ± 5.6	8.3 ± 4.1	6.9 ± 2.3	8.8 ± 1.5
Gasoline exhaust	41.5 ± 2.9	31.3 ± 8.3	31.3 ± 8.5	28.3 ± 12.3	33.1 ± 5.8
Diesel exhaust	0.0 ± 0.0	0.0 ± 0.0	1.0 ± 1.9	0.0 ± 0.0	0.2 ± 0.5
Distant sources	41.2 ± 7.0	29.8 ± 10.4	32.2 ± 7.2	46.0 ± 11.7	37.3 ± 7.6
City gas	0.0 ± 0.0	5.9 ± 1.8	3.3 ± 5.5	0.4 ± 0.9	2.4 ± 2.8
Solvent	2.6 ± 1.0	2.7 ± 1.4	4.0 ± 2.8	1.6 ± 0.8	2.7 ± 1.0
Biogenic	0.4 ± 0.1	1.7 ± 0.7	3.3 ± 1.4	0.4 ± 0.3	1.4 ± 1.4

Hellen, 2003

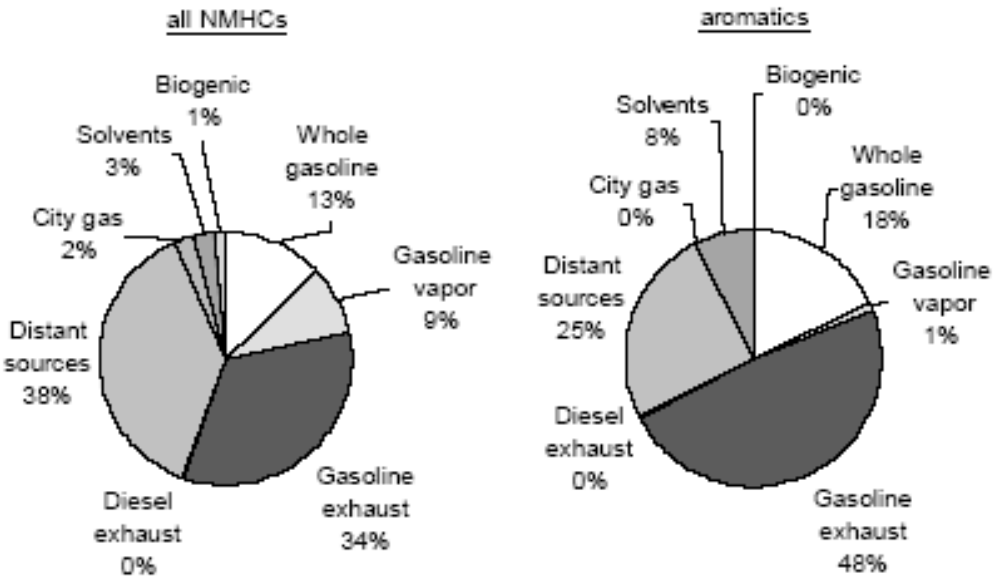

Fig. 1. CMB calculated contributions (% of measured mass) of different source categories of all NMHCs and aromatic compounds in Helsinki.

Hellen, 2003

ACP Mass Balance: inorganic data

Oyama, et al., (2016)

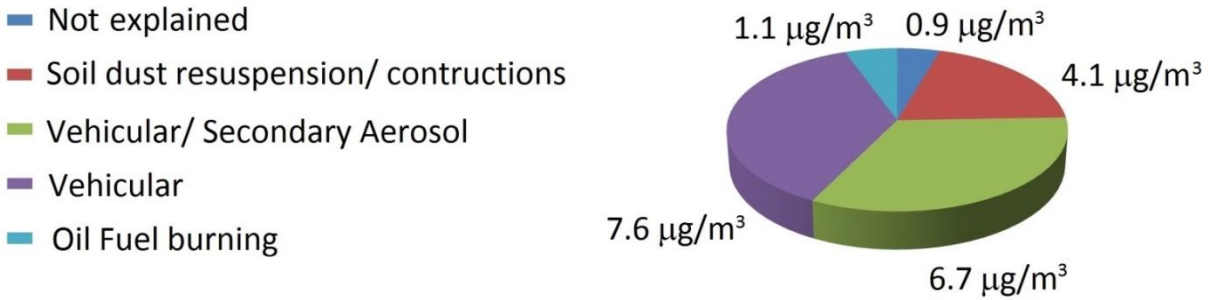

Vehicular emissions of organic particulate matter in Sao Paulo, Brazil
Author(s): B.S. Oyama et al.
MS No.: acp-2015-774, submitted

Andrade et al. (2012)

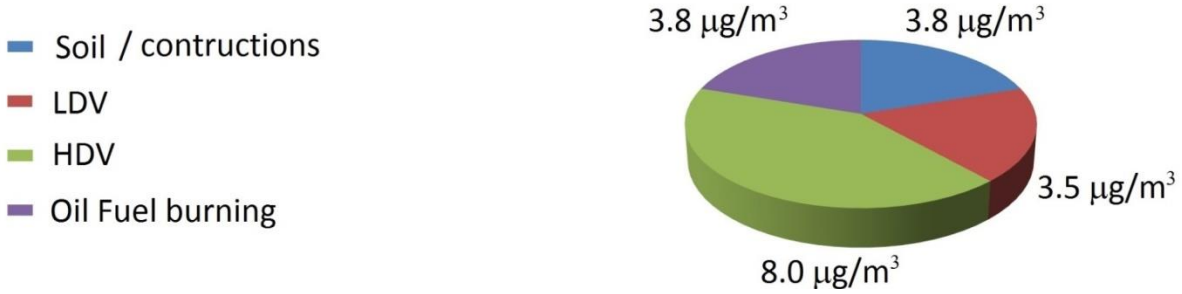

Andrade et al., 2012. Vehicle emissions and PM2.5 mass concentrations in six Brazilian Cities. Air Quality, Atmosphere & Health. Volume 5, 1, pp 79-88.

- Vehicular emissions: more than 60% and more than 50% (Andrade et al., 2012)

Example of project

Receptor Modeling: Identification of the vehicular emission contribution to $PM_{2.5}$ mass concentration in six Brazilian Cities

PROJECT:

Funded by the Ministry of

Environment

Coordination: Medical School USP

Região Metropolitana	População (milhões)	Território (mil km2)
São Paulo	19.9	7.9
Rio de Janeiro	11.8	5.6
Belo Horizonte	5.0	0.9
Porto Alegre	9.8	4.1
Curitiba	3.2	15.4
Recife	3.8	2.8

Recife

Belo Horizonte

Rio de Janeiro

São Paulo

Curitiba

Porto Alegre

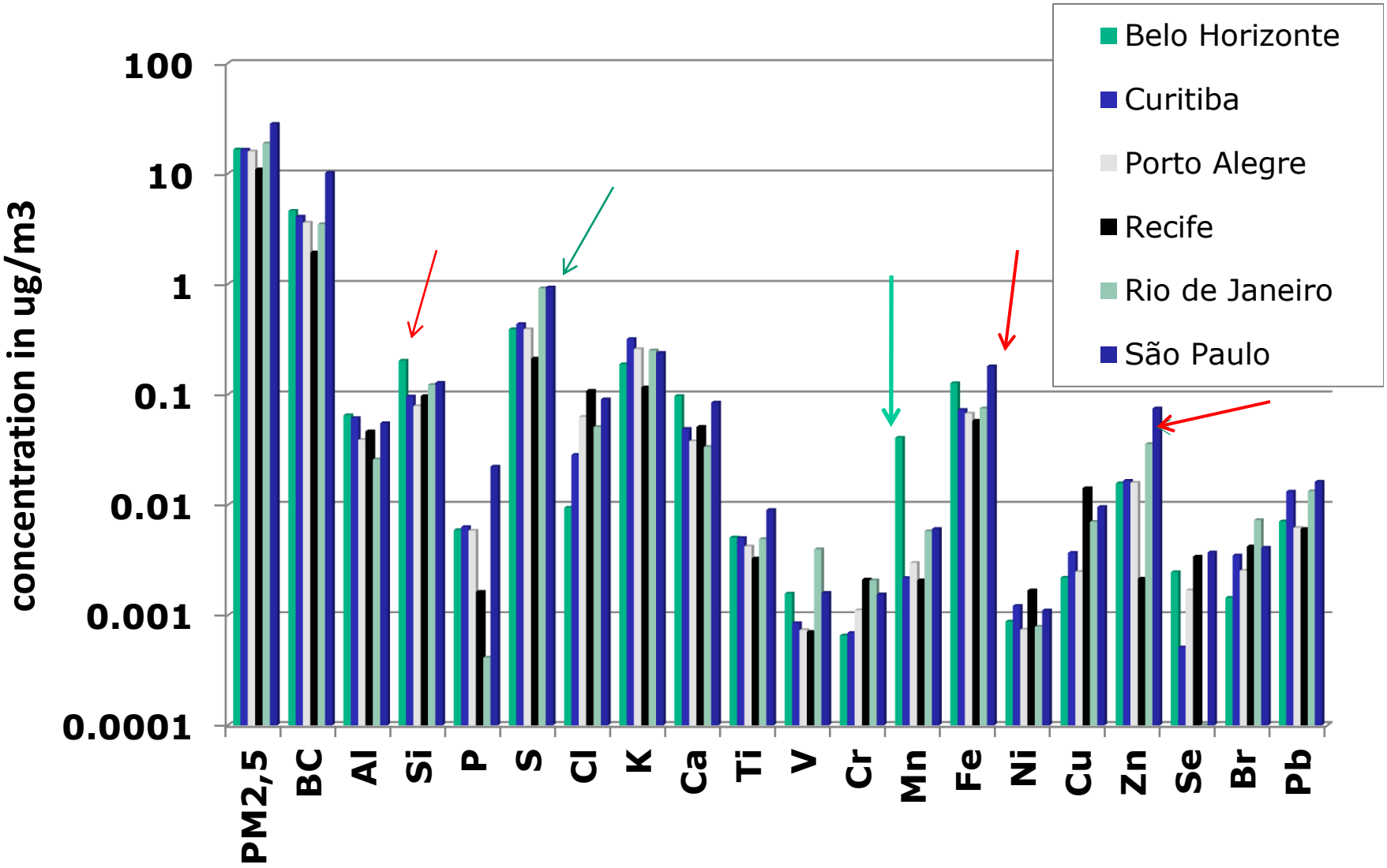
concentration in ug/m3
100
10
1
0.1
0.01
0.001
0.0001
PM2,5
BC
Al
Si
P
S
Cl
K
Ca
Ti
V
Cr
Mn
Fe
Ni
Cu
Zn
Se
Br
Pb
Belo Horizonte
Curitiba
Porto Alegre
Recife
Rio de Janeiro
São Paulo

Mean concentrations and standard deviations for PM2.5 and BC (in µg / m3) and for other elements in the fine fraction (in ng / m3). The loadings were obtained by VARIMAX rotation for Sao Paul based on the Maximum Likelihood Estimator of the covariance matrix.

	#Cases	Mean	Std.Dev.	Factor 1	Factor 2	Factor 3	Factor 4
$PM_{2.5}$	201	28.1	13.3	0.3813		0.4319	0.5924
BC	201	10.2	6.4			0.4483	0.6890
Al	160	55.2	61.5	0.9305			
Si	201	128.3	124.6	0.8728			
P	197	22.4	15.7		0.9185		
S	201	936.7	517.5		0.9464		
Cl	191	90.8	153.0			0.6049	0.4313
K	201	239.3	210.6				0.4525
Ca	201	84.9	88.6	0.8835			
Ti	201	9.0	8.8	0.8948			
V	193	1.6	1.2		0.7223		
Cr	188	1.6	1.6			0.8202	
Mn	200	6.1	4.1	0.4363		0.5870	0.4654
Fe	201	181.0	122.7	0.7088			0.4893
Ni	139	1.1	0.9			0.8772	
Cu	183	9.6	8.2			0.5056	0.6597
Zn	199	75.1	65.1				0.6925
Br	182	4.1	3.6				0.6736
Pb	162	16.3	13.0				0.8261
Eingenvalue				4.8	2.9	3.6	4.1
Explained variance (%)				26.7	15.9	20.2	22.9

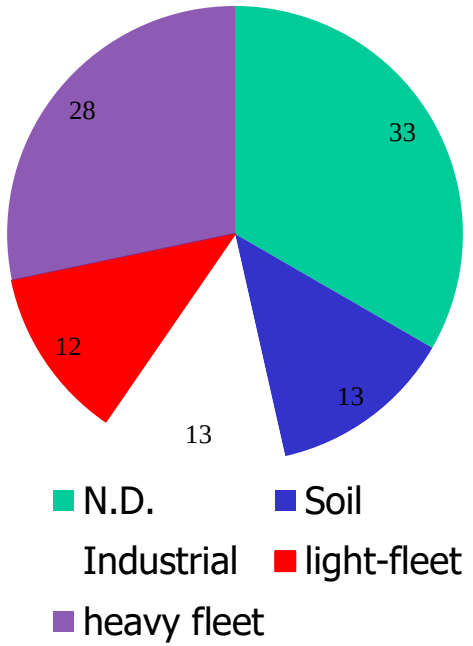

Sao Paulo

Mean concentrations and standard deviations for PM2.5 and BC (in µg / m3) and for other elements in the fine fraction (in ng / m3). The loadings were obtained by VARIMAX rotation Rio de Janeiro based on the Maximum Likelihood Estimator of the covariance matrix.

	#Cases	Mean	Std.Dev.	Factor 1	Factor 2	Factor 3	Factor 4	Factor 5
$PM_{2.5}$	150	17.2	11.1		0.8778			
BC	150	3.3	2.2		0.7073			0.4984
Al	125	49.8	58.8	0.8807				
Si	149	121.0	128.5	0.7847				
S	150	658.1	449.3		0.7146	0.4726		
Cl	137	51.9	81.2		0.5925			0.5293
K	149	177.7	166.5		0.7988			
Ca	148	41.4	35.8	0.8513				
Ti	150	5.6	4.8	0.9069				
V	149	4.3	2.6			0.8750		
Cr	147	1.8	0.7				0.8636	
Mn	148	4.2	2.5				0.6416	
Fe	150	75.3	55.2	0.7552	0.4090			
Ni	140	2.8	1.6			0.7801		
Cu	146	8.2	5.7					0.7752
Zn	149	24.7	21.5					0.6938
Br	150	6.4	4.2		0.6386			0.4525
Pb	149	12.2	10.1					0.8069
Eigenvalue				8.8	1.9	1.8	1.3	0.91
Explained Variance (%)				8.8	10.8	9.9	7.5	5.1

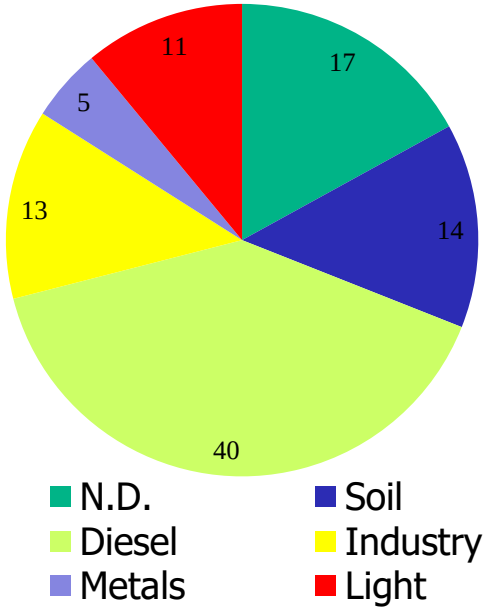

Rio de Janeiro

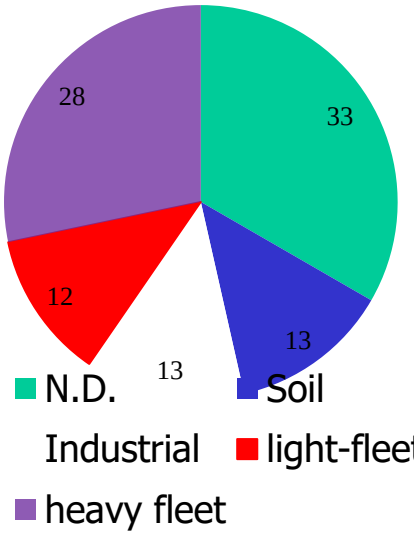

São Paulo

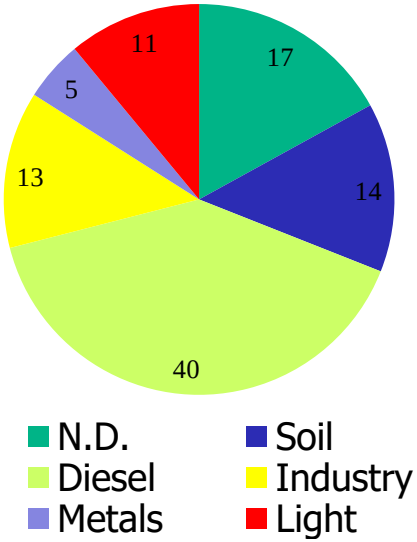

Rio de Janeiro

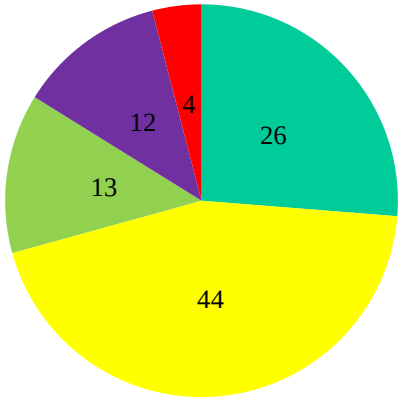

Belo Horizonte

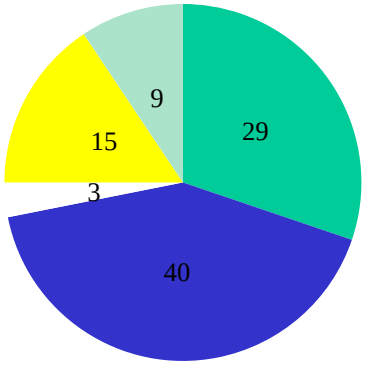

Curitiba

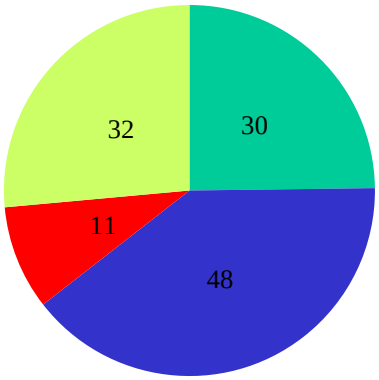

Porto Alegre

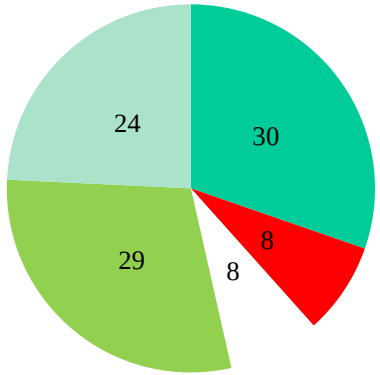

Recife

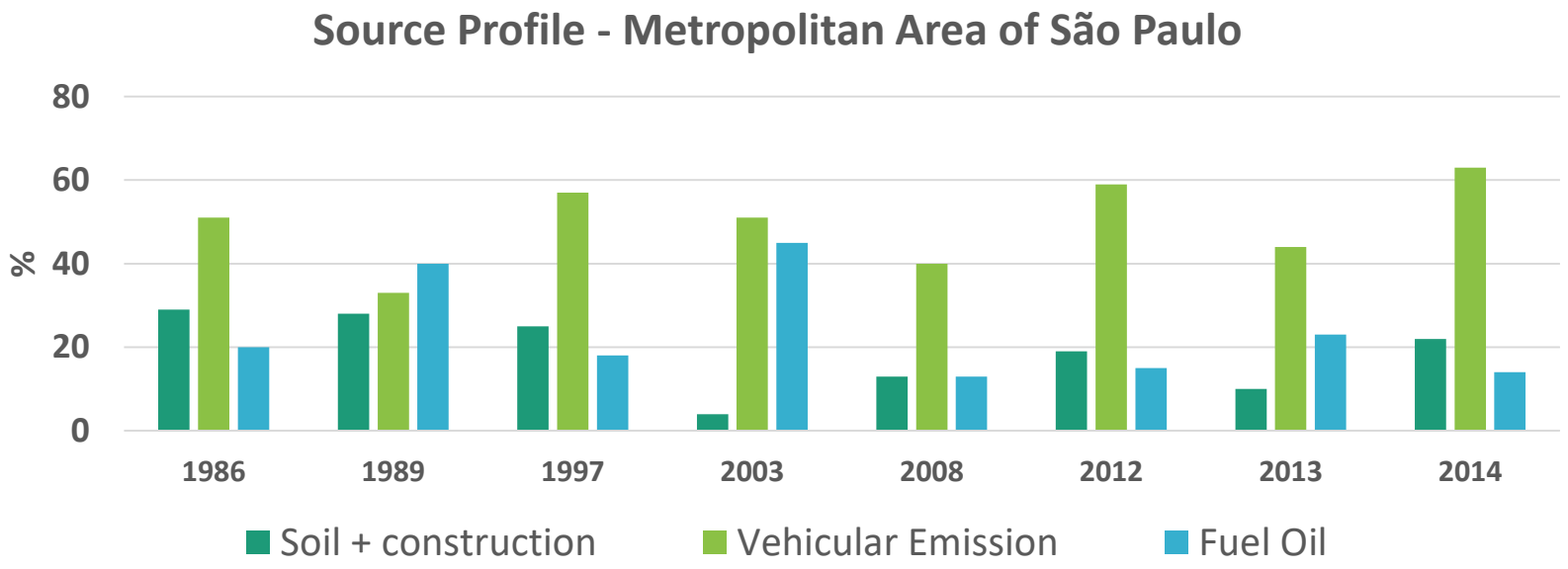

Receptor Modeling for São Paulo

- Results for 2012-2013-2014 from PMF
- Results from 1986 to 2008 with APCA
- The participation in the $PM_{2.5}$ has, in average increased for mobile source

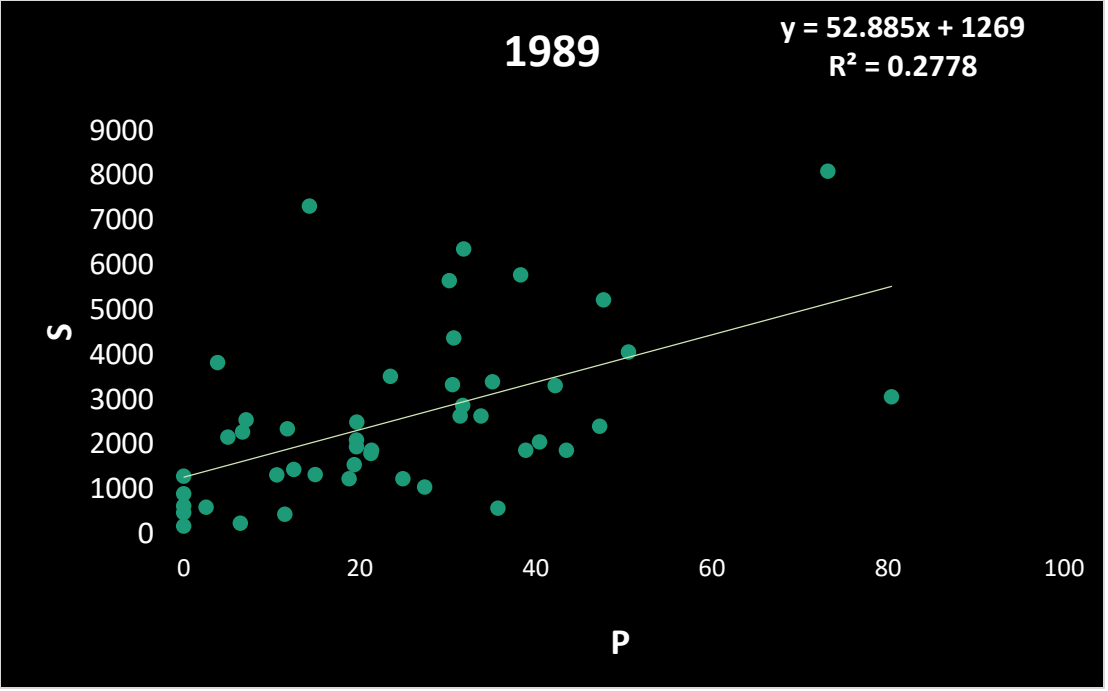

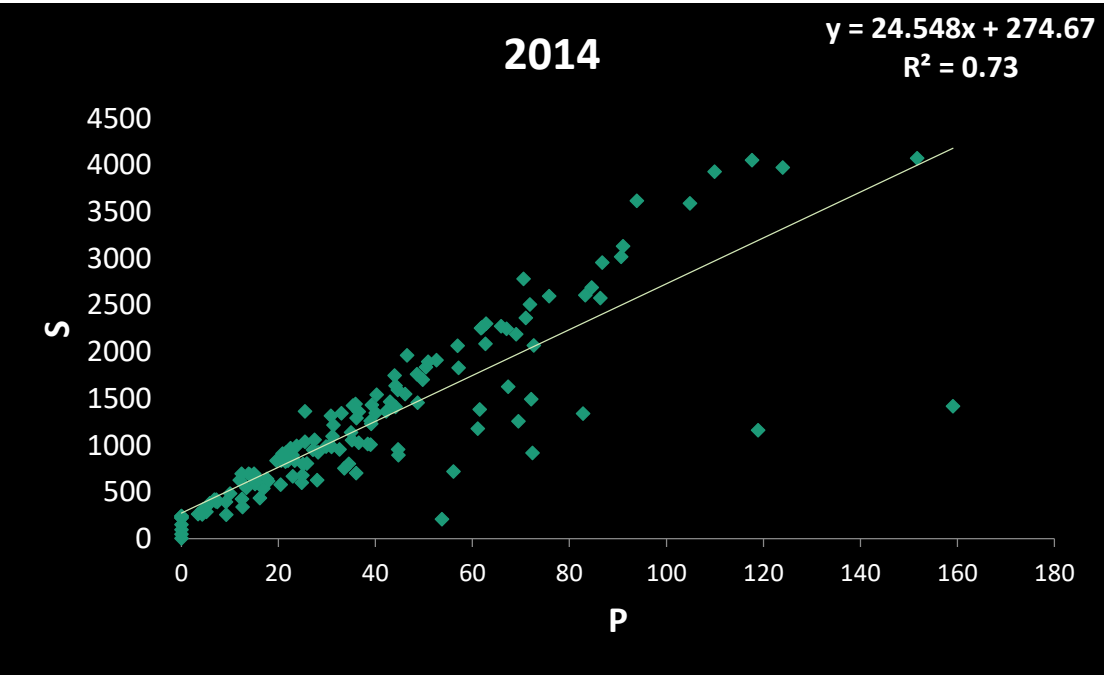

Which elements can be sources markers?

The sources tracers have been changing with time: a Strong correlation between S and P indicates the presence of mobile sources, mainly diesel.

We found the same profile at bus terminals and trucks garage.

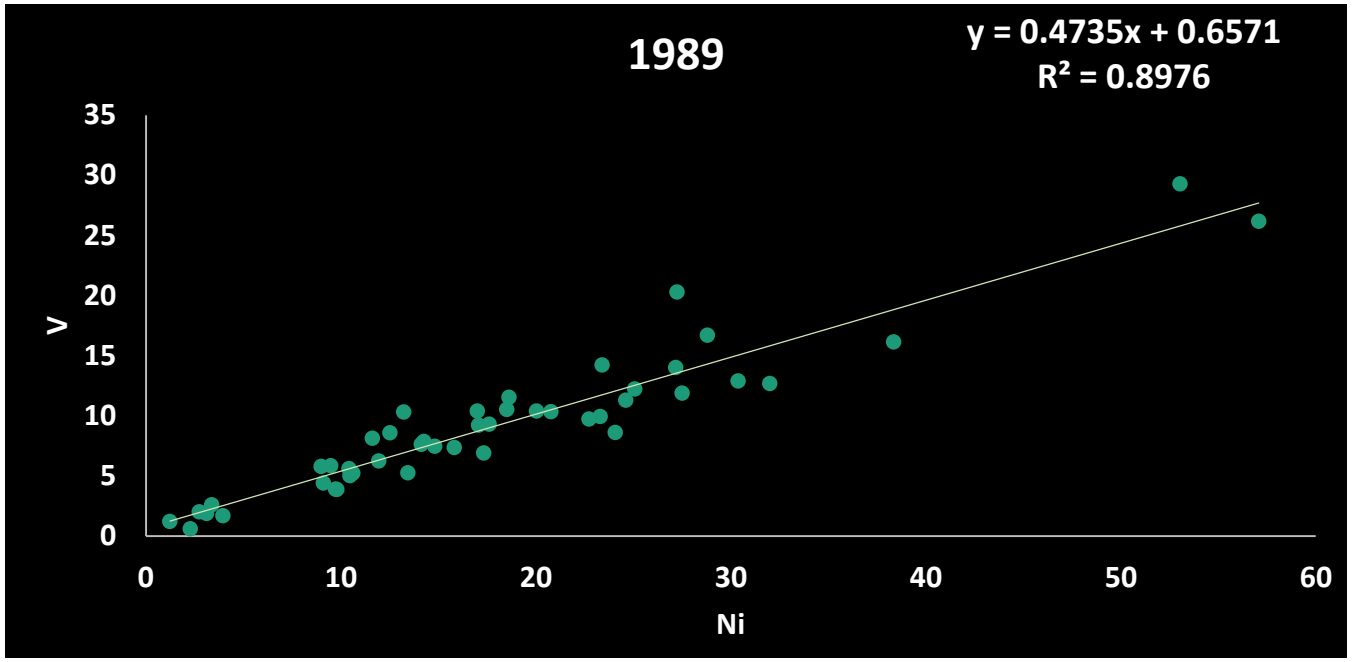

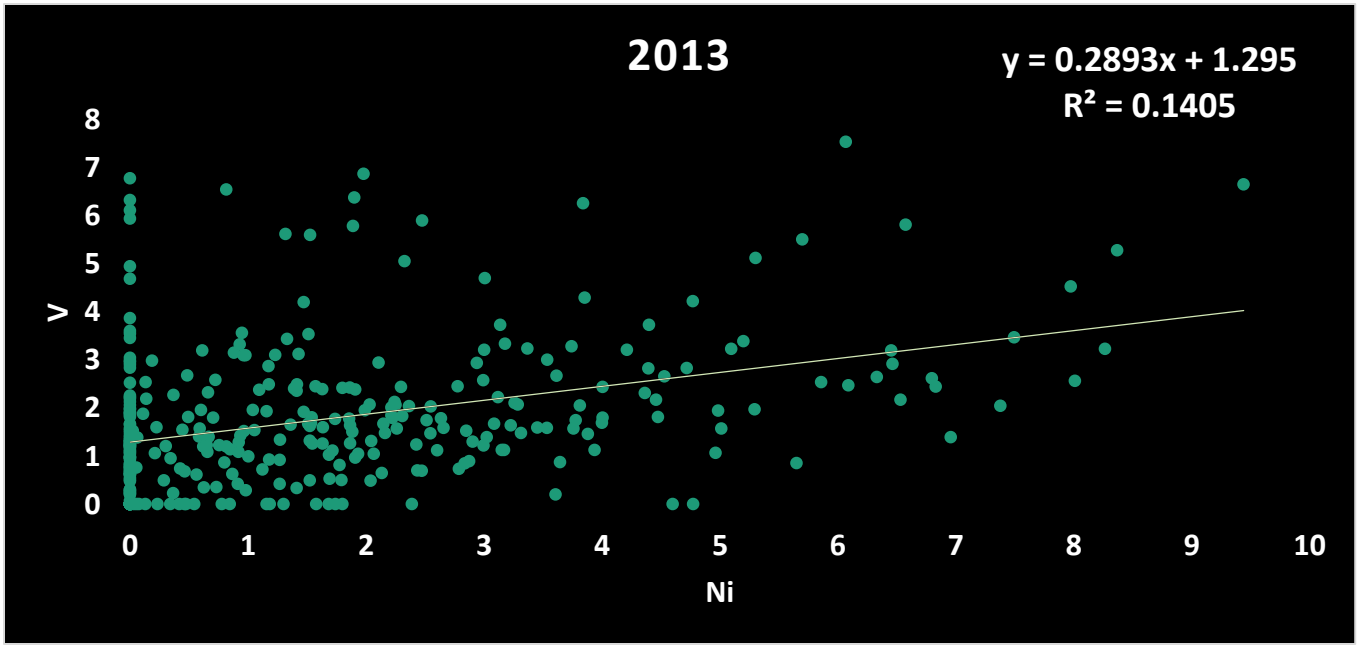

V and Ni, classical indicators of fuel burning are not presenting high correlation any more.

Positive Matrix Factorizaton (PMF)

Review on recent progress in observations, source identifications and countermeasures of $PM_{2.5}$

Chun-Sheng Liang [a,c], Feng-Kui Duan [a,**], Ke-Bin He [a,b,*], Yong-Liang Ma [a,b]

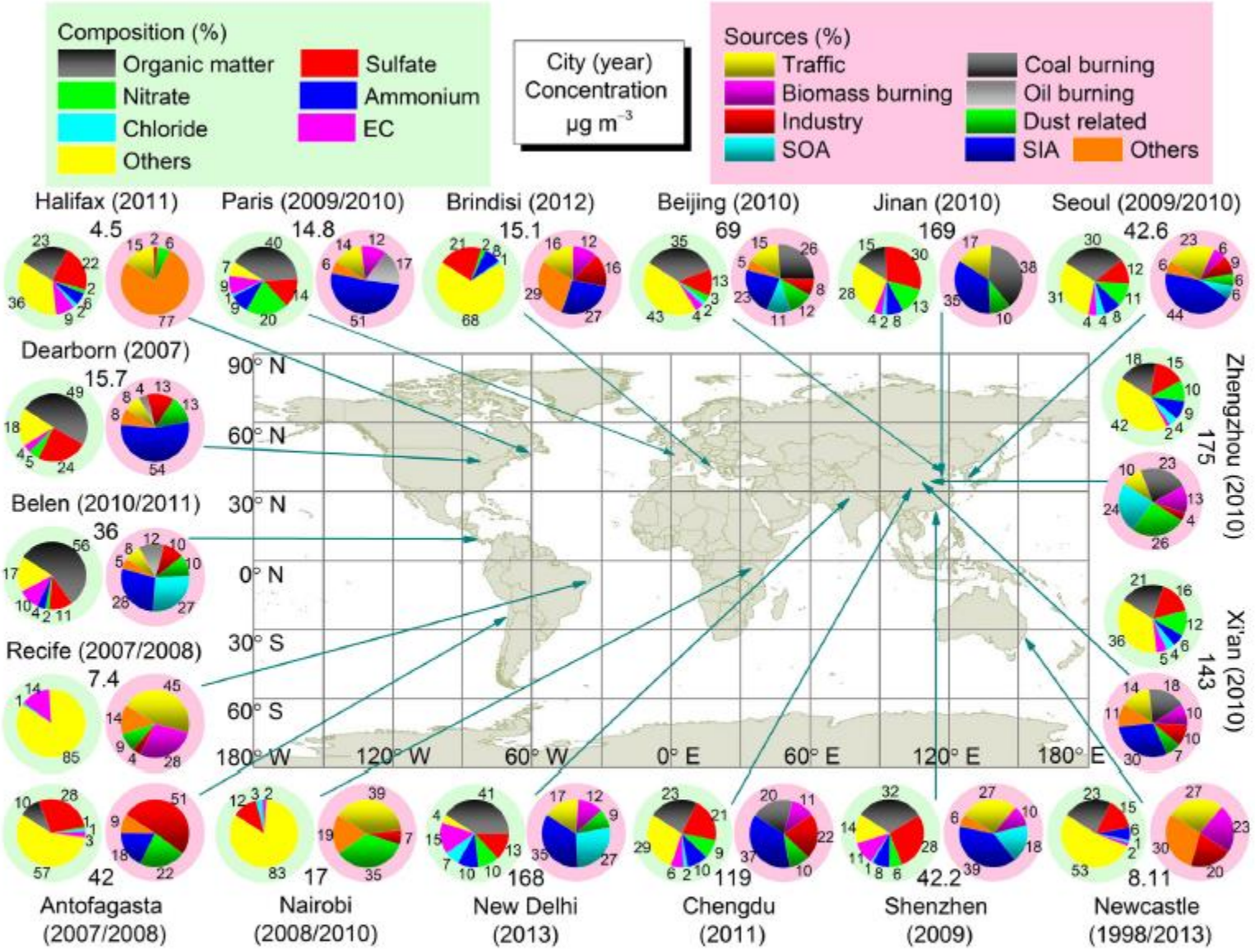

Fig. 2. Concentrations, composition and sources of $PM_{2.5}$ in different continents according to the recently reported results. Results were based on PMF, except in New Delhi (pragmatic mass closure). Data taken from references: Seoul (Choi et al., 2013), Beijing (Wu et al., 2014b), Jinan (Gu et al., 2014), Zhengzhou (Geng et al., 2013), Xi'an (Wang et al., 2015c), Chengdu (Tao et al., 2014a), Shenzhen (Huang et al., 2014b), New Delhi (Pant et al., 2015), Paris (Bressi et al., 2013; Bressi et al., 2014), Brindisi (Cesari et al., 2014), Halifax (Gibson et al., 2013), Dearborn (Pancras et al., 2013), Costa Rica (Murillo et al., 2013b), North Chile (Jorquera and Barraza, 2013), Recife (dos Santos et al., 2014), Nairobi (Gaita et al., 2014), Newcastle (Stelcer et al., 2014). See Table S3 for details.

PMF

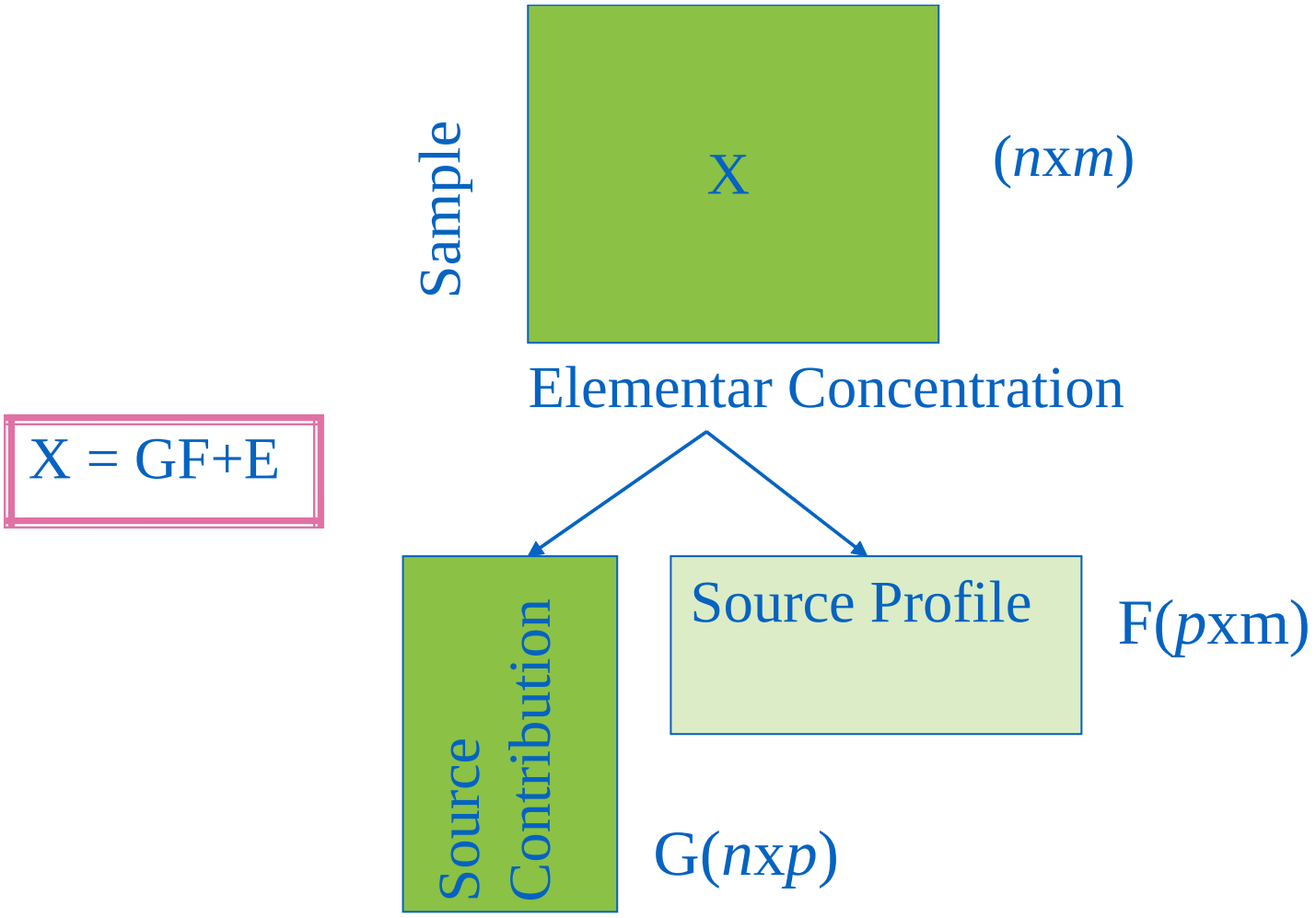
Sample
X
(nxm)
Elementar Concentration
X = GF+E
Source Contribution
G(nxp)
Source Profile
F(pxm)

PMF

$$E = X - Y = X - GF$$

$$e_{ij} = x_{ij} - y_{ij} = x_{ij} - \sum_{k=1}^{p} g_{ik} f_{kj} \; ;$$

$i = 1,\ldots..,n$ (i^{esima} sample)

$j = 1,\ldots..,m$ (j^{esimo} element)

$k = 1,\ldots..,p$ (k^{esima} source)

$$Q(E) = \sum_{i=1}^{n} \sum_{j=1}^{m} (e_{ij} / s_{ij})^2$$

; $g_{ik} > 0$ e $f_{kj} > 0$

s_{ij} = uncertainty de x_{ij}.

Factor contributions and profiles are derived by the PMF model minimizing the objective function Q (Equation 1-2):

$$Q = \sum_{i=1}^{n} \sum_{j=1}^{m} \left[\frac{x_{ij} - \sum_{k=1}^{p} g_{ik} f_{kj}}{u_{ij}} \right]^2$$

Q is a critical parameter for PMF and two versions of Q are displayed for the model runs.

- Q(true) is the goodness-of-fit parameter calculated including all points.
- Q(robust) is the goodness-of-fit parameter calculated excluding points not fit by the model, defined as samples for which the uncertainty-scaled residual is greater than 4.

PMF5.0 manual

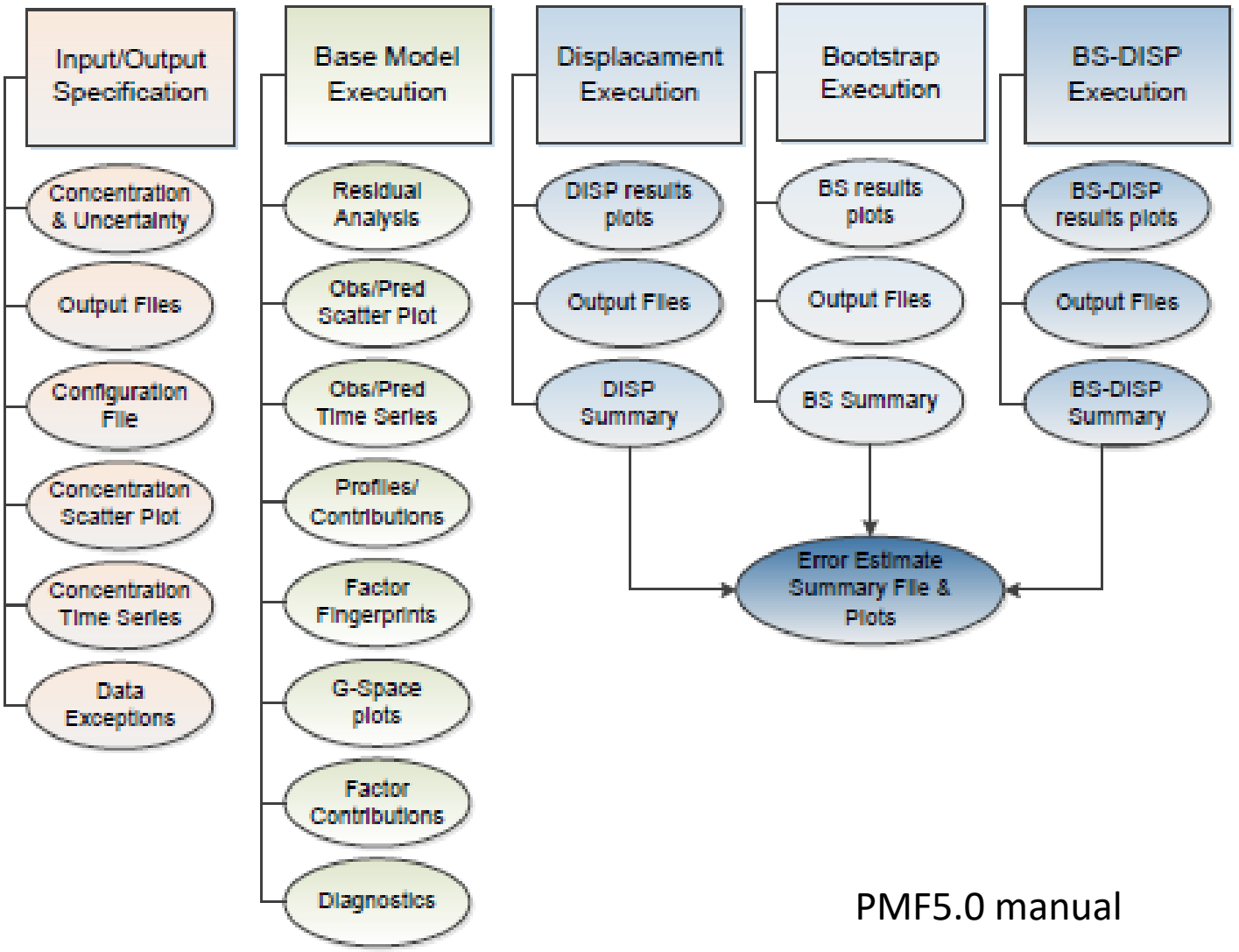

PMF5.0 manual

Figure 6. Flow chart of operations within EPA PMF – Base Model.

Two calculations are performed to determine S/N, where concentrations below uncertainty are determined to have no signal, and for concentrations above uncertainty, the difference between concentration (x_i) and uncertainty (s_i) is used as the signal (Equation 5-3):

$$d_{ij} = \left(\frac{x_{ij} - s_{ij}}{s_{ij}} \right) \quad \text{if } x_{ij} > s_{ij}$$

$$d_{ij} = 0 \qquad \text{if } x_{ij} \le s_{ij}$$

S/N is then calculated using Equation 5-4:

$$\left(\frac{S}{N} \right)_j = 1/n \sum_{i=1}^{n} d_{ij}$$

PMF5.0 manual

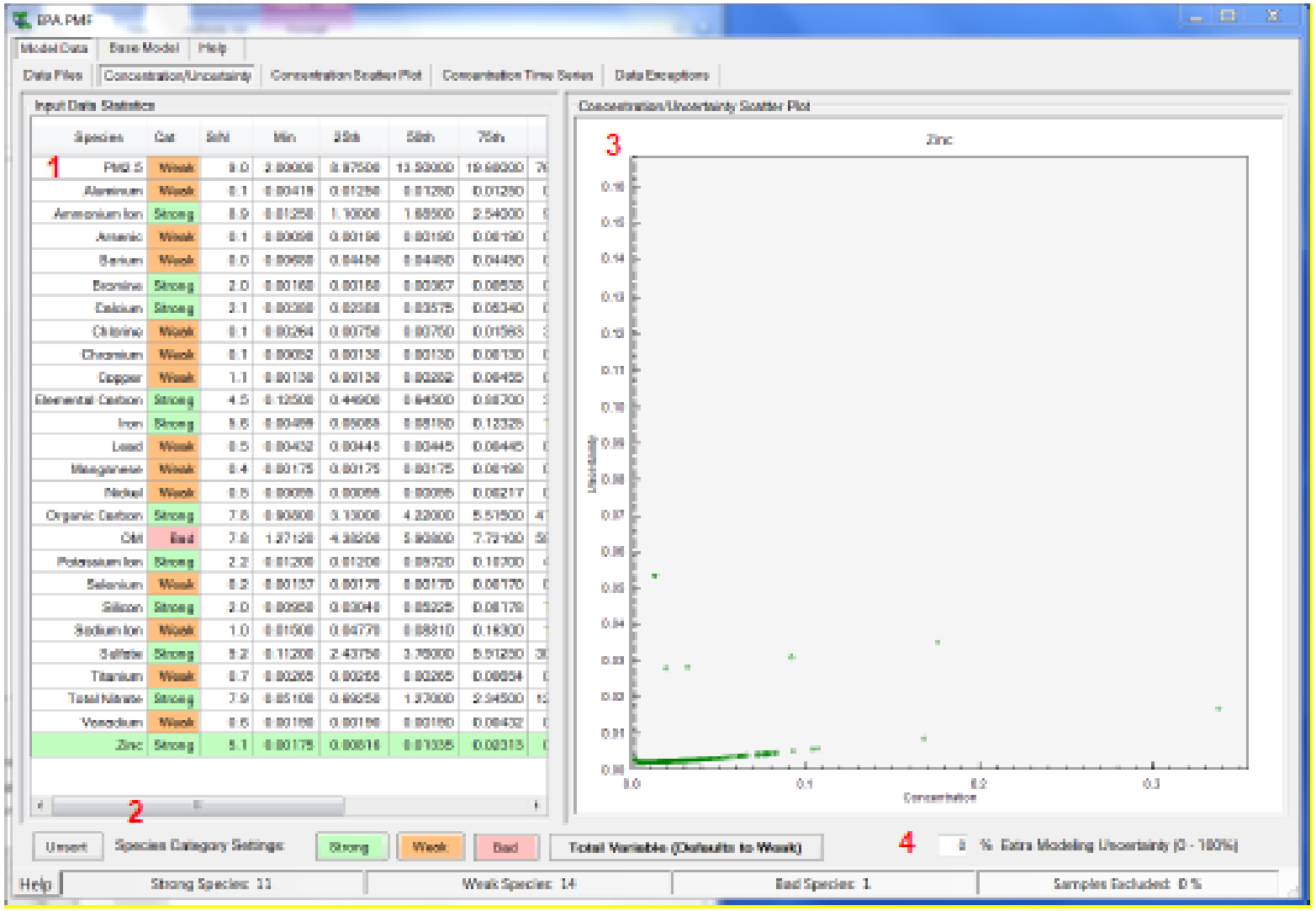

Figure 9. Example of the Concentration/Uncertainty screen.

Displacement (DISP) intervals include effects of rotational ambiguity. They do not include effects of random errors in the data. For modeling errors, if the user misspecifies the data uncertainty, DISP intervals are directly impacted.

Bootstrap (BS) intervals include effects from random errors and partially include effects of rotational ambiguity. For modeling errors, if the user misspecifies the data uncertertainty, BS results are still generally robust.

BS-DISP intervals include effects of random errors and rotational ambiguity. For modeling errors, if the user misspecifies data uncertainty, BS-DISP results are more robust than for DISP since the DISP phase of BS-DISP does not displace as strongly at DISP by itself.

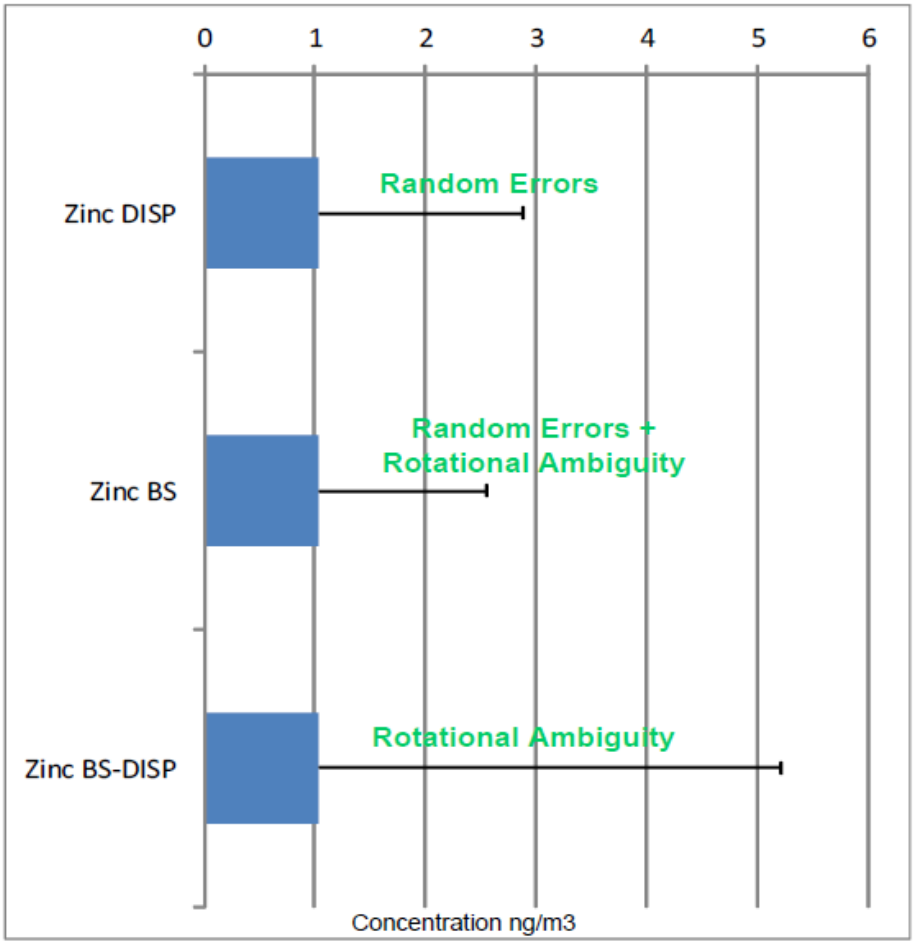

Figure 24. Comparison of upper error estimates for zinc source.

PMF5.0 manual

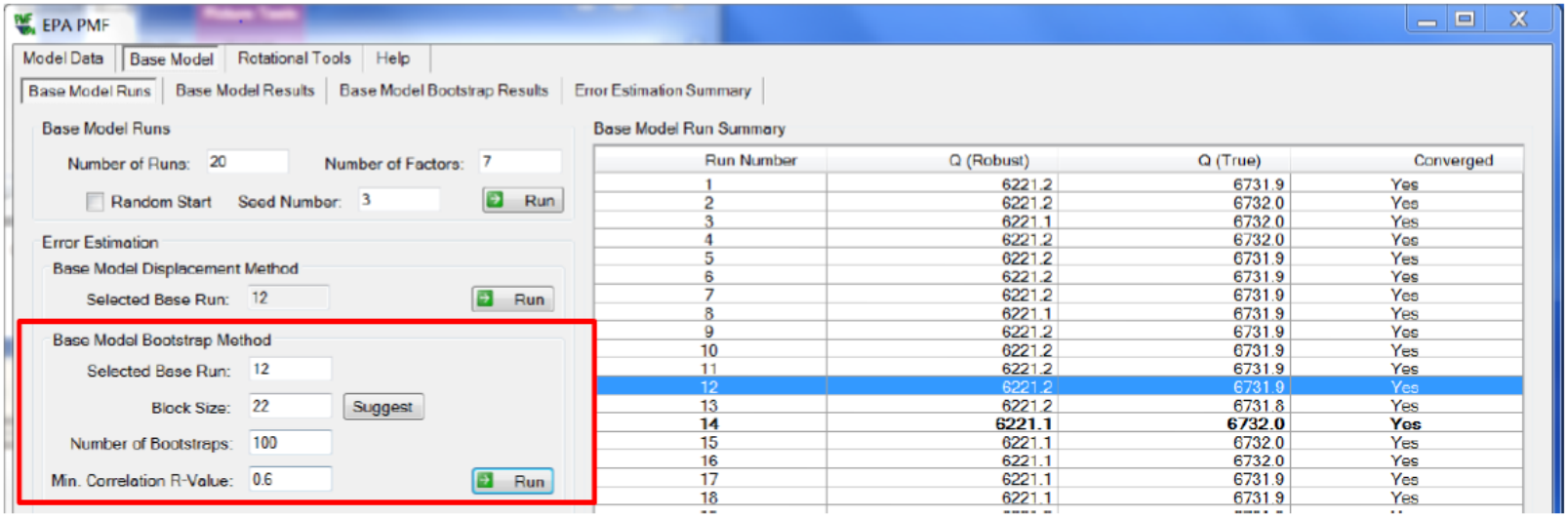

Figure 26. Example of the Base Model Runs screen highlighting the Base Model Bootstrap Method box.

Atmos. Chem. Phys., 17, 11943–11969, 2017
https://doi.org/10.5194/acp-17-11943-2017

Atmospheric Chemistry and Physics
Open Access
EGU

Particulate pollutants in the Brazilian city of São Paulo: 1-year investigation for the chemical composition and source apportionment

Guilherme Martins Pereira[1,4], Kimmo Teinilä[2], Danilo Custódio[1,3], Aldenor Gomes Santos[4,5,6], Huang Xian[7], Risto Hillamo[2], Célia A. Alves[3], Jailson Bittencourt de Andrade[4,5,6], Gisele Olímpio da Rocha[4,5,6], Prashant Kumar[8,9], Rajasekhar Balasubramanian[7], Maria de Fátima Andrade[10], and Pérola de Castro Vasconcellos[1,4]

Table 4. Average, minimum and maximum concentrations of tracer elements for all campaigns.

	$Int_{2.5}$	$Ext_{2.5}$	Ext_{10}
(ng.m^{-3})	Average (min–max)	Average (min–max)	Average (min–max)
Li	0.48 (< DL–1.12)	0.27 (< DL–0.70)	0.40 (< DL–1.23)
Mg	210 (5–469)	93 (5–356)	154 (< DL–377)
Al	1851 (< DL–2782)	691 (< DL–2712)	981 (< DL–3014)
K	1431 (191–3833)	300 (< DL–1967)	600 (< DL–1682)
Ca	1164 (< DL–3204)	397 (< DL–1671)	666 (< DL–2160)
Cr	23 (1–60)	13 (1–60)	20 (< DL–54)
Mn	30 (< DL–64)	17 (< DL–49)	33 (4–175)
Fe	962 (173–2056)	581 (140–1408)	1269 (240–3578)
Co	0.45 (0.03–1.06)	0.23 (0.01–0.78)	0.59 (0.07–1.74)
Ni	7.3 (2.3–14.8)	4.6 (< DL–16.1)	6.6 (< DL–25.9)
Cu	181 (7–390)	109 (7–308)	188 (32 –976)
Zn	284 (< DL–673)	110 (< DL–279)	193 (< DL–716)
As	2.8 (0.06–5.7)	1.9 (< DL–7.1)	2.2 (< DL–7.9)
Se	5.6 (< DL–13.2)	2.6 (< DL–7.5)	2.6 (< DL–7.9)
Rb	5.7 (0.4–12.3)	2.2 (0.1–8.9)	2.6 (0.2–8.9)
Sr	6.6 (0.4–13.4)	3.0 (0.2–12.2)	4.8 (0.4–14.3)
Cd	2.5 (0.2–15.1)	0.8 (0.1–3.0)	1.2 (0.2–10.6)
Sn	19.5 (3.2–40.2)	8.8 (0.3–35.9)	12.3 (1.6–41.8)
Cs	0.28 (0.07–1.01)	0.14 (< DL–0.51)	0.19 (0.02–0.77)
Tl	0.21 (< DL–0.75)	0.13 (< DL–0.38)	0.15 (0.03 –0.65)
Pb	54 (3–172)	31 (3–71)	42 (4–176)
Bi	0.76 (0.06–3.03)	0.47 (< DL–3.03)	0.83 (0.12–3.24)

< DL: below detection limit

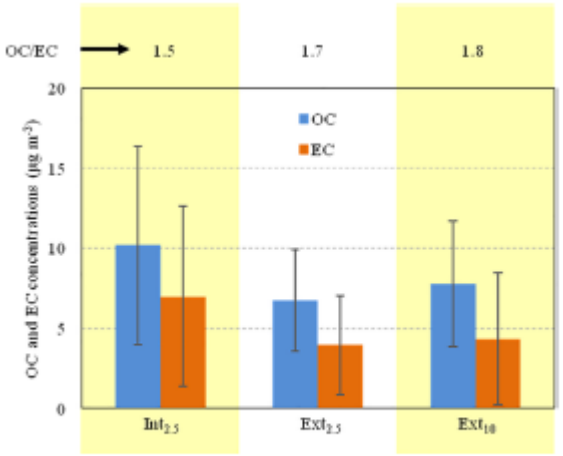

Figure 4. Carbonaceous species concentrations for all campaigns.

Pereira et al., 2017

Table S. Concentrations of PAHs and derivatives for all campaigns.

	$Int_{2.5}$	$Ext_{2.5}$	Ext_{10}
(ng m^{-3})	Average (min–max)	Average (min–max)	Average (min–max)
Nap	0.30 (0.17–0.77)	0.36 (0.02–0.77)	0.41 (0.09–0.81)
Acy	0.09 (0.06–0.12)	0.10 (0.03–0.19)	0.12 (0.05–0.34)
Ace	0.05 (0.02–0.08)	0.05 (0.02–0.16)	0.07 (0.02–0.23)
Fln	0.27 (0.15–1.03)	0.31 (0.06–1.44)	0.51 (0.10–1.75)
Phe	0.65 (0.30–2.48)	0.74 (0.12–3.55)	1.28 (0.28–4.08)
Ant	0.17 (0.10–0.44)	0.16 (0.06–0.60)	0.25 (0.08–0.67)
Flt	0.48 (0.21–0.86)	0.53 (0.06–1.40)	0.73 (0.19–2.21)
Pyr	0.52 (0.20–0.99)	0.54 (0.07–1.54)	0.71 (0.19–2.45)
BaA	1.0 (0.3–2.4)	0.9 (0.1–4.8)	1.2 (0.3–5.9)
Chr	1.8 (0.5–4.4)	1.6 (0.3–5.7)	2.1 (0.5–10.5)
BbF	3.0 (0.9–6.1)	2.3 (0.5–6.4)	3.0 (0.7–13.3)
BkF	2.5 (0.6–5.2)	1.9 (0.2–7.4)	2.5 (0.4–11.8)
BeP	2.8 (0.6–6.1)	2.2 (0.3–7.3)	2.8 (0.5–14.4)
BaP	2.3 (0.4–5.5)	1.6 (0.2–7.6)	2.0 (0.3–12.5)
Per	0.35 (0.04–0.79)	0.27 (< DL–1.27)	0.38 (0.05–1.90)
InP	2.9 (0.6–6.0)	1.8 (0.3–6.3)	2.4 (0.4–13.2)
DBA	0.8 (0.1–2.3)	0.6 (0.0–2.0)	0.9 (0.0–5.1)
BPe	2.4 (0.5–4.8)	1.6 (0.2–5.5)	2.1 (0.4–10.5)
Cor	1.0 (0.1–2.4)	0.7 (0.0–2.4)	0.9 (0.1–5.2)
Total	23.3 (6.0–48.8)	18.4 (2.6–61.6)	24.3 (5.4–115.3)
BaPE	3.4 (0.6–8.0)	2.4 (0.3–10.5)	3.2 (0.5–18.3)
1-NNap	< DL	< DL	< DL
1-Methyl-4-NNap	< DL	< DL	< DL
2-NNap	< DL	< DL	< DL
2-NBP	0.56 (< DL–1.36)	0.56 (< DL–1.36)	1.23 (0.47–2.47)
1-Methyl-5-NNap	0.18 (< DL–0.28)	< DL	< DL
1-Methyl-6-NNap	0.36 (< DL–0.40)	0.27 (< DL–0.41)	0.29 (< DL–0.86)
2-Methyl-4-NNap	0.45 (< DL–0.45)	0.36 (< DL–0.44)	0.42 (< DL–1.26)
3-NBP	0.60 (0.48–0.88)	0.52 (< DL–0.87)	0.55 (< DL–1.38)
4-NBP	< DL	< DL	0.18 (< DL–0.41)
5-NAce	< DL	< DL	0.20 (< DL–0.52)
2-NFln	0.98 (0.78–1.39)	0.99 (0.38–1.56)	1.09 (0.54–1.79)
2-NPhe	0.43 (0.30–0.67)	0.51 (0.19–1.40)	0.61 (< DL–1.80)
3-NPhe	0.43 (< DL–0.46)	0.44 (< DL–0.68)	0.47 (< DL–1.11)
9-NPhe	0.62 (< DL–0.64)	0.52 (< DL–0.64)	0.55 (< DL–0.82)
2-Nant	0.66 (< DL–0.80)	0.56 (< DL–0.80)	0.61 (< DL–0.88)
9-Nant	0.44 (< DL–0.57)	0.42 (< DL–0.69)	0.46 (< DL–1.15)
2-NFlt	1.19 (< DL–1.35)	0.98 (< DL–1.25)	1.02 (< DL–1.43)
3-NFlt	1.45 (< DL–1.48)	1.05 (< DL–1.48)	1.02 (< DL–1.11)
1-NPyr	0.98 (< DL–1.12)	0.73 (< DL–0.88)	0.79 (< DL–1.28)
2-NPyr	0.94 (< DL–0.99)	0.76 (< DL–0.99)	0.78 (< DL–1.27)
4-NPyr	1.61 (< DL–1.67)	1.27 (< DL–1.34)	1.28 (< DL–1.72)
7-NBaA	1.19 (< DL–1.34)	0.91 (< DL–1.06)	1.01 (< DL–1.67)
6-NChr	< DL	0.60 (< DL–0.67)	0.69 (0.58–1.10)
3-NBA	< DL	< DL	< DL
6-NBaPyr	< DL	< DL	1.01 (< DL–1.19)
1-NBaPyr	< DL	< DL	< DL
3NBePyr	< DL	< DL	< DL
1,4-BQ	< DL	< DL	< DL
1,4-NQ	0.54 (0.43–0.72)	0.44 (0.28–0.67)	0.46 (0.31–1.08)
1,2-NQ	< DL	< DL	< DL
9,10-AQ	1.6 (0.8–3.7)	2.5 (0.3–8.0)	2.6 (0.4–10.9)
9,10-PQ	< DL	< DL	< DL
Total PAHs / OC (%)	0.23	0.27	0.31
ΣLMW / ΣHMW	0.32	0.41	0.43
Flt /(Flt+Pyr)	0.5	0.5	0.5
BaA / Chr	0.5	0.6	0.5
InP / (InP+BPe)	0.5	0.5	0.5
BaP /(BaP+BeP)	0.4	0.4	0.4
BPe /BaP	1	1	1
2-NFlt / 1-NPyr	1.3	1.3	1.3

Pereira et al., 2017

Atmos. Chem. Phys., 17, 11943–11969, 2017 www.atmos-chem-phys.net/17/11943/2017/

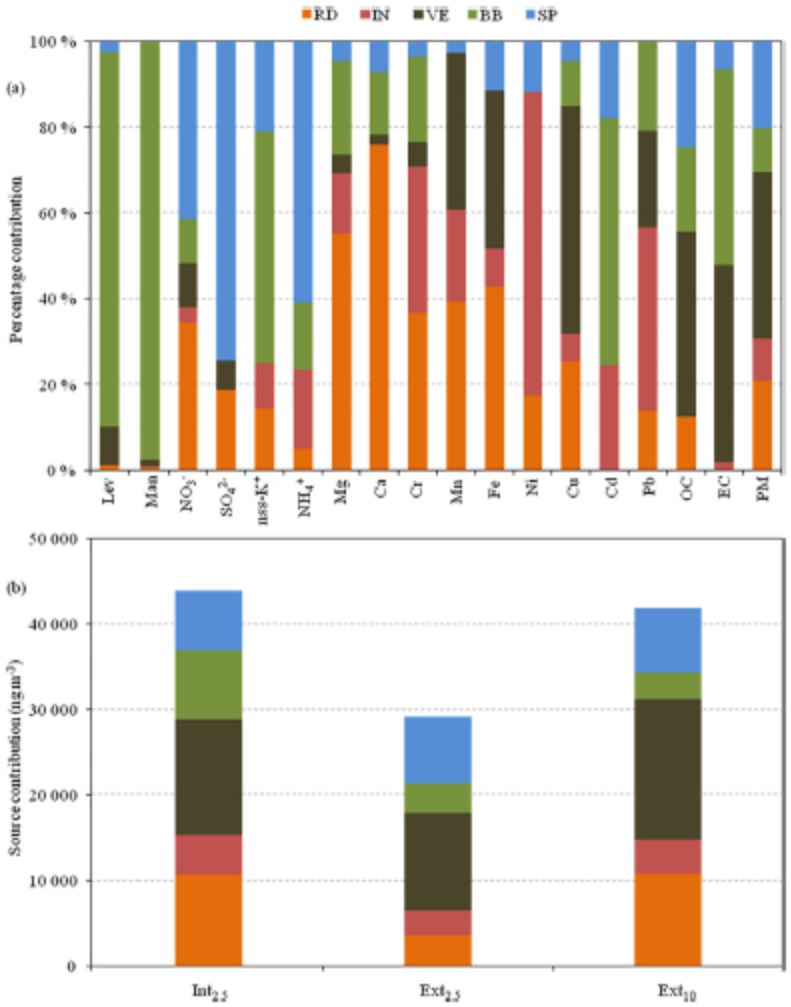

Figure 9. (a) Profile of species for each source (RD – road dust, IN – industrial, VE – vehicular, BB – biomass burning and SP – secondary processes). (b) Contribution of sources for each campaign.

Pereira et al., 2017

Example

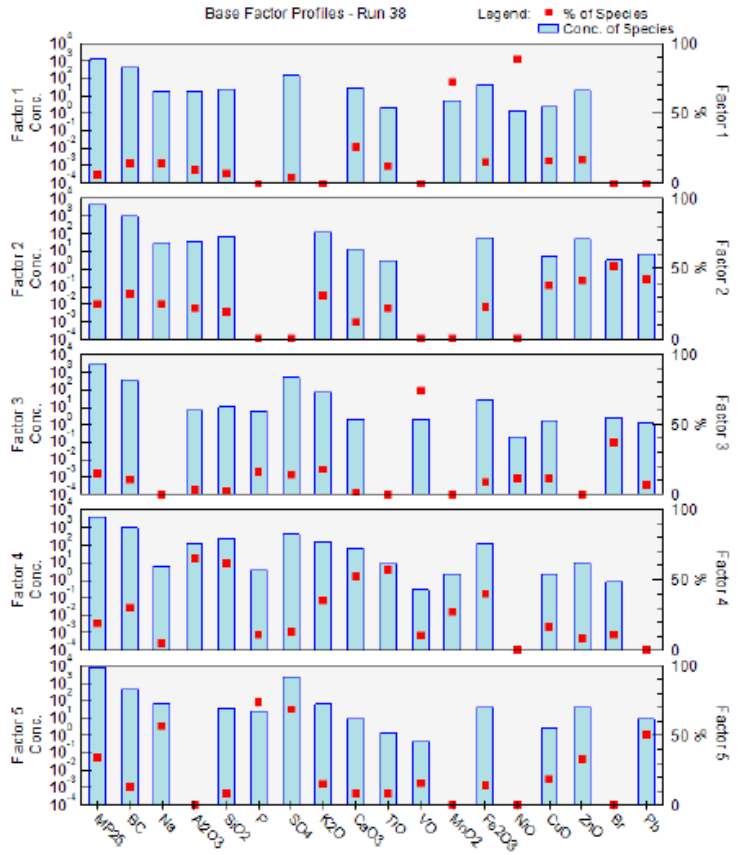

Figura 4.4: Perfis das fontes obtidas pelo PMF, em % de massa dos compostos (quadrado vermelho) e concentração em ng/m³ (histograma em azul), para os dados do ano de 2012.

Tabela 4.5: Identificação de cada fator encontrado no PMF, seus elementos traçadores e sua contribuição na massa do $MP_{2,5}$ para os dados do ano de 2012.

Fator	Traçadores	Fonte	Participação (%)
1	Mn, Ni	Industrial	6,6
2	$MP_{2,5}$, BC, K, Cu, Zn, Br, Pb	Veicular	24,8
3	V, Br	Veículos leves	14,8
4	Al, Si, Ca, Ti e Fe	Solo	19,5
5	$MP_{2,5}$, Na, P, S, Zn, Pb	Veicular	34,3

Dissertação Yann Marien, 2017

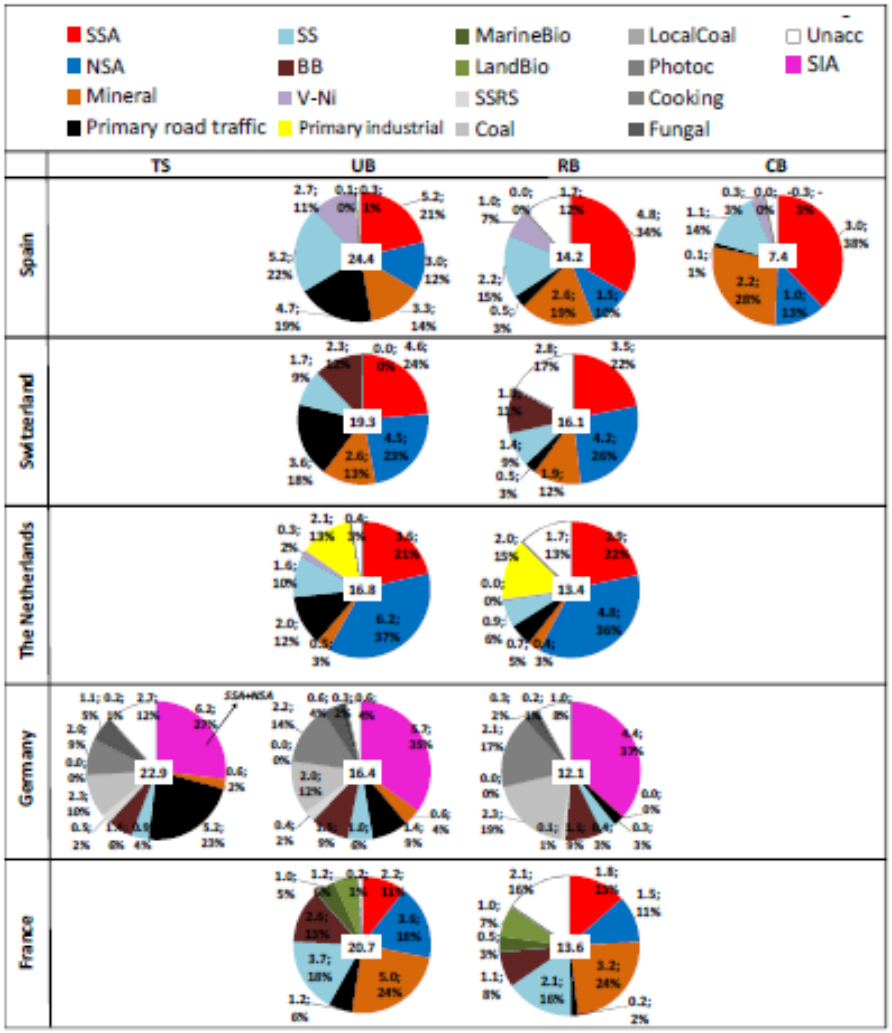

Figure 2: Mean annual source contributions to PM_{10} ($PM_{2.5}$ for NL) from the multi-site PMF for each country. The number in the white box at the center of the pie chart is the measured mass of PM (in $\mu g/m^3$). TS: traffic site; UB: urban background; RB: regional background; CB: continental background.

Long range and local air pollution: what can we learn from chemical speciation of particulate matter at paired sites?

Marco Pandolfi [*,*], Dennis Mooibroek [b], Philip Hopke [c], Dominik van Pinxteren [d], Xavier Querol [*], Hartmut Herrmann [d], Andrés Alastuey [*], Olivier Favez [e], Christoph Hüglin [f], Esperanza Perdrix [g], Véronique Riffault [g], Stéphane Sauvage [g], Eric van der Swaluw [b], Oksana Tarasova [h], and Augustin Colette [e]

https://doi.org/10.5194/acp-2019-493
Preprint. Discussion started: 18 June 2019

Atmos. Chem. Phys. Discuss., https://doi.org/10.5194/acp-2019-74
Manuscript under review for journal Atmos. Chem. Phys.
Discussion started: 15 April 2019

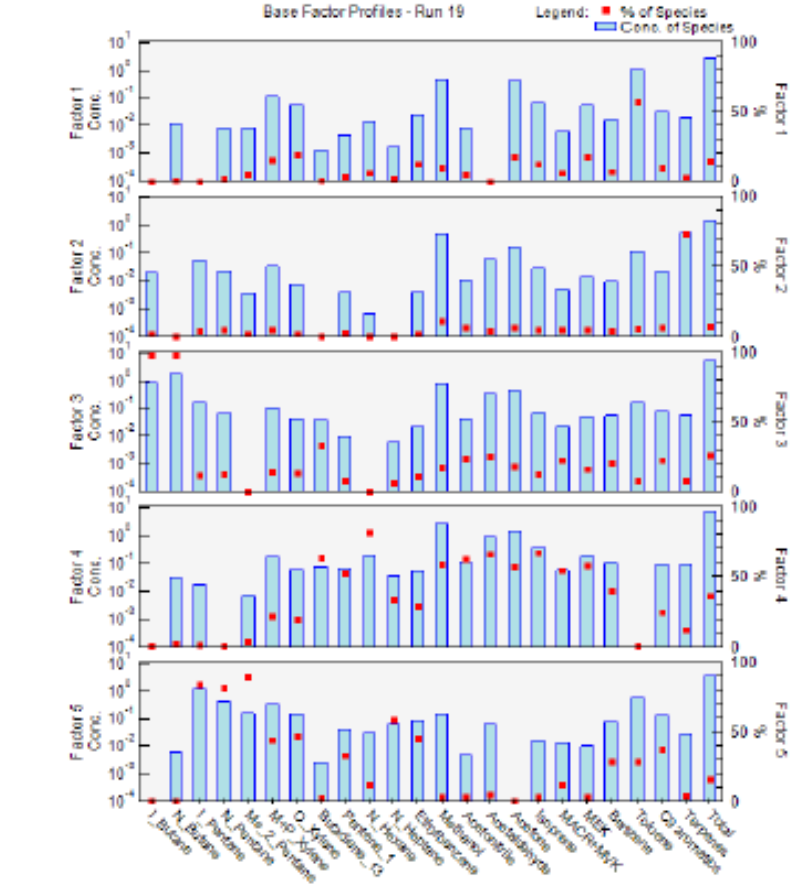

Figure 6: Source composition profiles of the PMF factors. The concentrations (ppbv) and the percent of each species apportioned to the factor are displayed as a pale blue bar and a red color box, respectively.

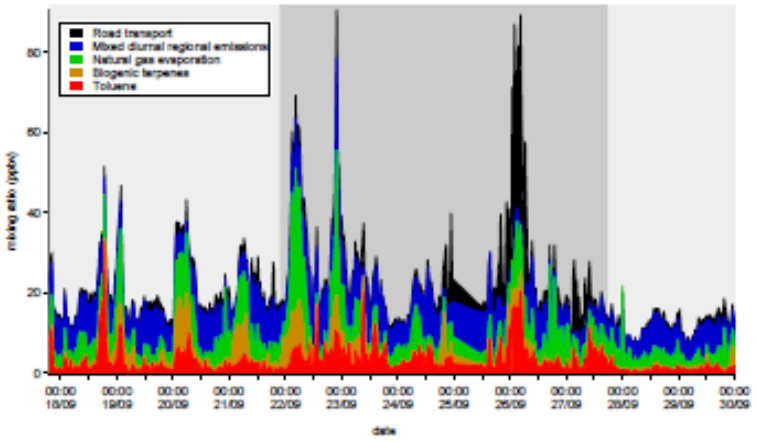

Figure 7: Time series of factor contributions (in ppbv) extracted from the PMF.

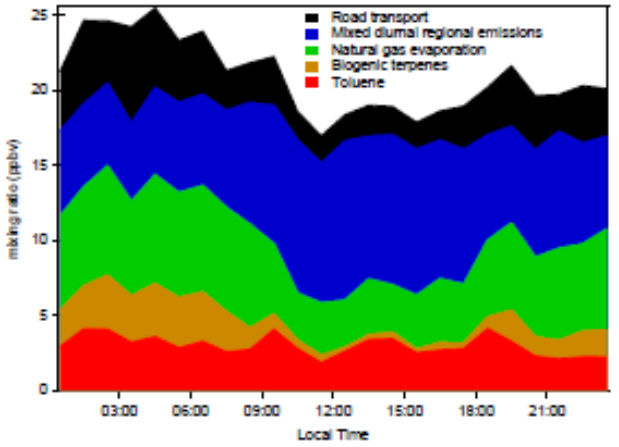

Figure 8: Diurnal variation of source contribution (in ppbv)

Istambul, port region.

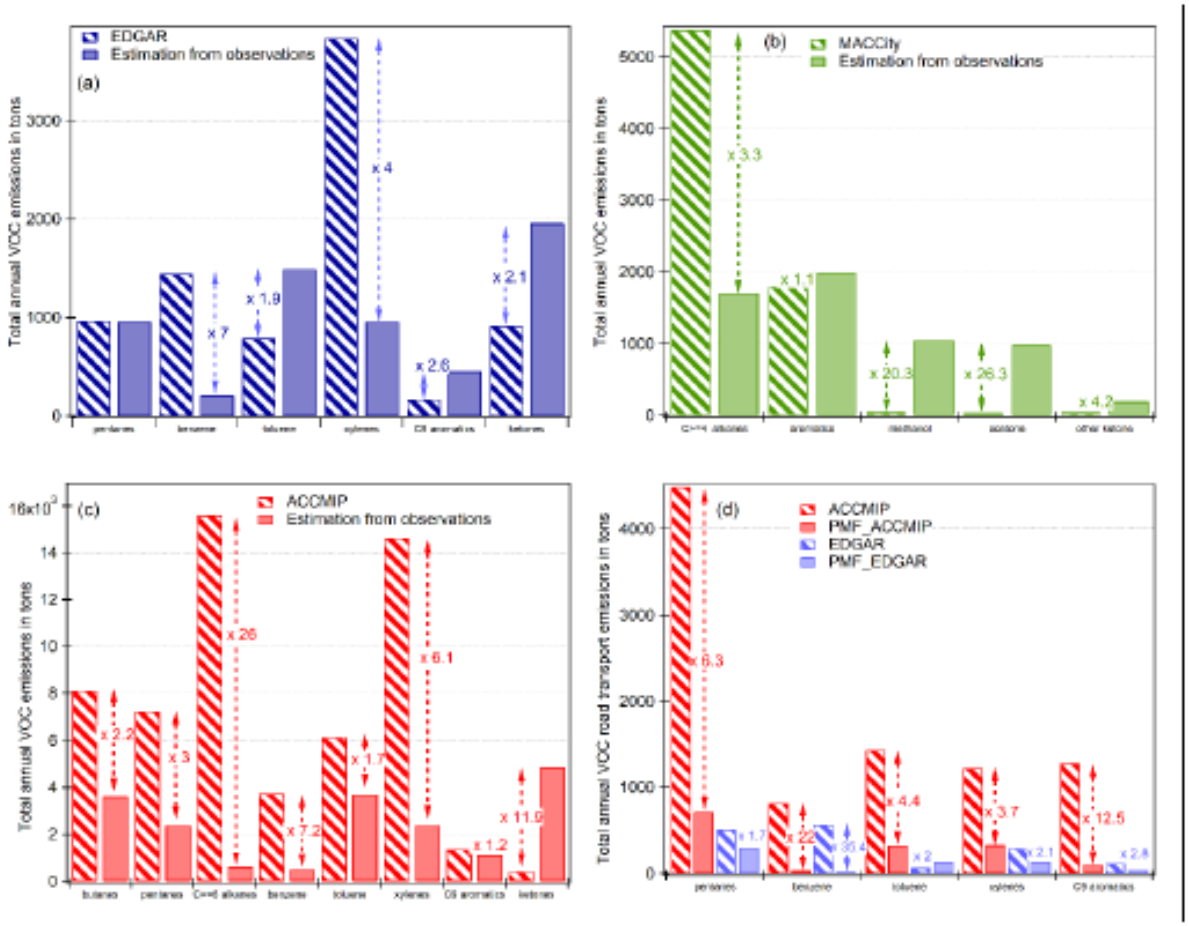

)00 **Figure 11: Comparison of the estimated emissions inventory from observations and PMF results and global emission inventories : a) EDGAR, b) MACCity, c) ACCMIP, d) Road transport for ACCMIP and EDGAR inventory.**

Composition and variability of gaseous organic pollution in the port megacity of Istanbul: source attribution, emission ratios and inventory evaluation

Conclusions

- The analysis of trace-concentration variations with time can indicate the importance of specific sources
- The elemental composition of particulate matter can represent the variation in the role to specific source to atmospheric concentration
- The combination of different receptor models (Principal Component Analysis and Positive Matrix Factorization) is recommended to indirectly include the correlation analysis in the identification of sources through the tracers of the sources.

References:

1) Philip K. Hopke (2016) Review of receptor modeling methods for source apportionment, Journal of the Air & Waste Management Association, 66:3, 237-259, https://doi.org/10.1080/10962247.2016.1140693

2) Baye T.P. Thera1, Pamela Dominutti2, Fatma Öztürk3, Thérèse Salameh4, Stéphane 5 Sauvage4, et al., Composition and variability of gaseous organic pollution in the port megacity of Istanbul: source attribution, emission ratios and inventory evaluation. Atmos. Chem. Phys. Discuss., https://doi.org/10.5194/acp-2019-74

3) Marco Pandolfi a,*, Dennis Mooibroek et al.. Long range and local air pollution: what can we learn from chemical speciation of particulate matter at paired sites? https://doi.org/10.5194/acp-2019-493. Preprint. Discussion started: 18 June 2019

4) Chun-Sheng Liang, Feng-Kui Duan, Ke-Bin He, Yong-Liang Ma, Review on recent progress in observations, source identifications and countermeasures of PM2.5, Environment International, Volume 86, 2016, Pages 150-170, https://doi.org/10.1016/j.envint.2015.10.016.

5) C.A. Belis, F. Karagulian, B.R. Larsen, P.K. Hopke, Critical review and meta-analysis of ambient particulate matter source apportionment using receptor models in Europe, Atmospheric Environment, Volume 69, 2013, Pages 94-108, https://doi.org/10.1016/j.atmosenv.2012.11.009.

6) Andréa D.A. Castanho, Paulo Artaxo, Wintertime and summertime São Paulo aerosol source apportionment study, Atmospheric Environment, Volume 35, Issue 29, 2001, Pages 4889-4902, https://doi.org/10.1016/S1352-2310(01)00357-0.
7) Ivan Gregorio Hetem andMaria De Fatima Andrade · Characterization of Fine Particulate Matter Emitted from the Resuspension of Road and Pavement Dust in the Metropolitan Area of São Paulo, Brazil. *Atmosphere* 2016, *7*(3), 31; https://doi.org/10.3390/atmos7030031
8) Guilherme Martins Pereira, Kimmo Teinilä, Danilo Custódio, Aldenor Gomes Santos, Huang Xian, Risto Hillamo, Célia A Alves, Jailson Bittencourt de Andrade, Gisele Olímpio da Rocha, Prashant Kumar, Rajasekhar Balasubramanian, Maria de Fátima Andrade, Pérola de Castro Vasconcellos. Particulate pollutants in the Brazilian city of São Paulo: 1-year investigation for the chemical composition and source apportionment. Atmospheric Chemistry and Physics Discussions, 2017.
9) Pedro J Pérez-Martínez, Regina M Miranda, Thiago Nogueira, Maria L Guardani, Adalgiza Fornaro, R Ynoue, Maria F Andrade. Emission factors of air pollutants from vehicles measured inside road tunnels in São Paulo: case study comparison. International Journal of Environmental Science and Technology, 2014

Obrigada!
THANK YOU!

Acknowledgements